

CYCLIC OXIDATION BEHAVIOUR AND CHARACTERIZATION OF HVOF SPRAYED WC-NiCrFeSiB COATING

A DISSERTATION

*Submitted in partial fulfillment of the
requirements for the award of the degree*

of

MASTER OF TECHNOLOGY

In

METALLURGICAL & MATERIALS ENGINEERING

(With Specialization in Industrial Metallurgy)

By

AJAY MALIK



**DEPARTMENT OF METALLURGICAL & MATERIALS ENGINEERING
INDIAN INSTITUTE OF TECHNOLOGY ROORKEE
ROORKEE -247 667 (INDIA)
JUNE, 2006**

CANDIDATE'S DECLARATION

This is to certify that the work which is being hereby presented by me in this Dissertation titled **“Cyclic Oxidation Behaviour and Characterization of HVOF Sprayed WC-NiCrFeSiB coating.”** in Partial fulfillment of the award of the **Master of Technology** submitted at the Department of Metallurgical and Materials Engineering, IIT Roorkee, is a genuine account of my work carried out during the period from May 2005 to June 2006 under the guidance of **Dr. Satya Prakash & Dr. S.K.Nath**, Department of Metallurgical and Materials Engineering, IIT Roorkee.

The matter embodied in the project report to the best of my knowledge has not been submitted for the award of any other degree elsewhere.

Dated: *26.6.2006*


Ajay Malik

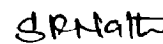
This is to certify that the above declaration by Ajay Malik is true to the best of my knowledge.


26.06.06

Dr. Satya Prakash

Professor

&



Dr. S.K.Nath

Professor

Department of Metallurgical and Materials Engineering

Indian Institute of Technology Roorkee

ROORKEE-247667 (INDIA)

ACKNOWLEDGEMENTS

I am deeply indebted to Dr. Satya Prakash and Dr. S.K. Nath for their constant and invaluable support, without which this project could not have been a reality. Their constant encouragement and helpful suggestions motivated me to work to the best of my abilities. My zeal and enthusiasm was kept alive by their steady faith in my aptitude.

I am grateful to Dr. P. S. Mishra, Head, Department of Metallurgical and Materials Engineering, IIT Roorkee, for providing me the necessary facilities to complete my dissertation work.

I am also highly obliged to Head, Institute Instrumentation Centre (IIC), Indian Institute of Technology Roorkee and Mrs. Rekha Sharma for extending necessary facilities during the experimental work.

I take this opportunity to thank Mr. Ramesh, Research Scholar for providing constant feedback at each stage of my project. The discussions I had with him led to timely and successful completion of the work.

In preparing the project, I have been fortunate to receive valuable assistance, suggestions, and support from Research Scholars Mr. Mahesh, Mr. T. S. Sidhu and Mr. Pawan Sapra for which I will always be grateful to them.

I am also thankful to Mr. Rajendra Sharma and Mr. Sethji for providing necessary facilities on time without which the project could not have reached such ends.

Ajay Malik
M.Tech II year
Metallurgical and Materials Engineering
June 2006

SYNOPSIS

Superalloys are used in turbines, boilers and coal conversion plants. From the application point of view, mechanical strength of oxide scales, growth stresses in the scales, oxide spallations and the loss of scale adherence to the substrate represent important factors in the determining the usefulness of metals and alloys as high temperature construction materials. It is their application at high temperature which makes the study of their behaviour at high temperature much more important. HVOF coating technology is capable of depositing a very wide range of compositions without significantly heating the substrate.

The present work is a comparative study of HVOF sprayed WC-NiCrFeSiB coating on a Ni-based superalloy (SN 75) and Fe-based superalloy (800H) in the different environments, such as simple oxidation (in presence of air only) and a molten salt environment (of 75% Na₂SO₄-25%NaCl) at 800 °C under cyclic conditions. Oxidation studies were conducted on uncoated superalloys as well. The thermo gravimetric technique was used to establish the kinetics of corrosion. X-ray diffraction, scanning electron microscopy analysis and electron probe microanalysis techniques were used to characterize the as sprayed coatings and corrosion products. The bare superalloys, in general, suffered accelerated corrosion under the given environmental conditions and showed spalling/sputtering of the oxide scale. The hot corrosion resistance of Ni-based superalloys was found to be better than that of Fe-based superalloys. The WC-NiCrFeSiB coating was found to be very effective in decreasing the corrosion rate in the given molten salt environment at 800 °C. The hot corrosion resistance imparted by WC-NiCrFeSiB coatings may be attributed to the formation of oxides of chromium and nickel and spinels of nickel and chromium.

Table of Contents

	<i>Page</i>
Candidate's Declaration	ii
Acknowledgements	iii
Synopsis	iv
Table of Contents	v
List of Figures	vii
List of Tables	ix
Chapter	
1. Introduction	1
2. Literature Survey	3
2.1. Hot Corrosion	3
2.2. Mechanisms of Hot Corrosion	5
2.3. High Temperature Oxidation Kinetics	7
2.4. Hot Corrosion of Superalloys	8
2.5. Protective Coating	11
2.5.1 Considerations in Coating Selection	12
2.6. Thermal Spray Coating	14
2.6.1 High Velocity Oxy Fuel Coatings	15
3. Problem Formulation	19
4. Experimental Procedure	21
4.1 Substrate Material	21
4.2 Sample Preparation	21
4.3 Coating Formulation	22
4.4 Molten Salt Corrosion Tests	22
4.5 Sources of Error	24
4.6 Precautions	25

5. Results	26
5.1 Uncoated Specimens	26
5.1.1 Hot Corrosion Study	26
5.1.1.1 Visual Inspection	26
5.1.1.2 Oxidation Kinetics	26
5.1.2 Characterization of Corrosion Products	29
5.1.2.1 X-ray Diffraction Analysis of Scales	29
5.1.2.2 SEM Analysis of Scale	30
5.1.2.3 Cross-sectional analysis of Oxide Scale	33
5.2 Coated Specimens	34
5.2.1 Hot Corrosion Study	34
5.2.1.1 Visual Inspection	34
5.2.1.2 Corrosion Kinetics	34
5.2.2 Characterization of Corrosion Products	36
5.2.2.1 X-ray Diffraction Analysis of Scales	36
5.2.2.2 SEM Analysis of Coating	38
5.2.2.3 SEM Analysis of Scale	39
5.2.2.4 Cross-sectional analysis of Oxide Scale	44
6. Discussion	50
7. Conclusion	53
Suggestions for Future Work	54
References	55

LIST OF FIGURES

<i>Number</i>	<i>Description</i>	<i>Page</i>
2.1	Schematic diagram of the HVOF coating process.	17
2.2	Characteristics of HVOF and standard plasma sprayed coatings.	18
5.1	Study of Corrosion Kinetics of bare superalloys.	27
5.2	(Weight gain / area) ² vs number of cycles plot for bare Superalloys.	27
5.3	XRD of bare superalloys in presence of molten salt environment.	29
5.4	XRD of bare superalloys after air oxidation.	30
5.5	SEM of uncoated Superfer 800 H after corrosion in molten salt environment.	31
5.6	SEM of uncoated Superni 75 after corrosion in molten salt environment.	32
5.7	BSE images of Uncoated Superfer 800 H after Hot corrosion.	33
5.8	BSE images of Uncoated Superni 75 after Hot corrosion.	33
5.9	Study of Corrosion Kinetics of coated superalloys.	35
5.10	(Weight gain / area) ² vs number of cycles plot for Coated Superalloys.	35
5.11	XRD of coated superalloys exposed to molten salt environment.	37
5.12	XRD of coated superalloys after simple air oxidation.	37
5.13	SEM of as sprayed coating.	38
5.14	SEM of coated Superfer 800 H after corrosion in molten salt environment.	40
5.15	SEM of coated Superni 75 after corrosion in molten salt environment.	41
5.16	SEM of coated Superfer 800 H after simple air oxidation.	42
5.17	SEM of coated Superni 75 after simple air oxidation.	43
5.18	BSE images of coated Superfer 800 H after corrosion in molten salt environment.	44

5.19 BSE images of coated Superni 75 after corrosion in molten salt environment.	45
5.20 BSE images of coated Superfer 800 H after air oxidation.	45
5.21 BSE images of coated Superni 75 after air oxidation.	45
5.22 EPMA of corroded WC-NiCrFeSiB coated Superfer 800 H in molten salt environment.	46
5.23 EPMA of corroded WC-NiCrFeSiB coated Superni 75 in molten salt environment.	47
5.24 EPMA of corroded WC-NiCrFeSiB coated Superfer 800 H after air oxidation.	48
5.25 EPMA of corroded WC-NiCrFeSiB coated Super 75 after air oxidation.	49
6.1 Cumulative weight gain of all the specimens.	52

LIST OF TABLES

<i>Number</i>	<i>Description</i>	<i>Page</i>
4.1	Nominal chemical composition (wt %) of substrate material.	21
4.2	Chemical composition of feedstock powders, particle size.	22
5.1	Values of Parabolic rate constant K_p for Bare superalloys.	28
5.2	Values of Parabolic rate constant K_p for WC-NiCrFeSiB coated superalloys.	36

Metals and alloys sometimes experience accelerated oxidation when their surfaces are covered by a thin film of fused salt in an oxidizing atmosphere at elevated temperatures. This mode of attack is called "hot corrosion", where a porous non protective oxide scale is formed at the surface and sulfides in the substrate. Hot corrosion is a term used for localized accelerated attack due to the presence of a salt layer on the metal, it is for instance observed on the blades and vanes of gas turbines.[1]

Hot corrosion has been observed in boilers, internal combustion engines, gas turbines, fluidized bed combustion and industrial waste incinerators since the 1940's. However, it became a topic of importance and popular interest in the late 1960's when gas turbine engines in military aircraft suffered severe corrosion during the Vietnam conflict while operating over sea water [2,3].

The loss due to corrosion of metals are very severe and from the economic point of view they are not comparable to any other losses. According to the recent estimates, corrosion of metal cost the united states over \$300 billion per year and it is more than the costs of annual floods and fires. Apart from these 40% of the total US steel production goes to the replacement of corroded parts and products. So far as India is concerned, corrosion cost is around Rs. 24000 crore due to materials corrosion in building structure, bridges, chemical plants etc. So it is important to understand the nature of all types of environment degradation of metals and alloys so that preventive measures against metal loss and failures can be economically devised to ensure safety and reliability in the use of metallic components. Although corrosion problems cannot be completely remedied, it is estimated that corrosion related cost can be reduced by more than 30% with the development and use of better corrosion control technologies [4].

The use of WC-based thermal spray coatings has been increasing in several areas due to their potentially high erosion and erosion–corrosion resistance. The potential for increased component lifetime can be attractive with respect to reducing maintenance costs as well as decreasing downtime. The increased demand for, and improvement of, thermal spray coatings are, in part, also due to continuous development and improvement in thermal spray technology, which is producing third generation coatings with minimum porosity and high bond strength [5].

The coating alloy selected for this study was WC–NiCrFeSiB composite powder which was sprayed using the HVOF process. The rationale of choosing this powder over other wear resistant materials currently used in different industrial applications resides in a number of special properties brought to the system by the powder constituents, e.g. tungsten carbide brings the wear resistance, nickel brings excellent wettability which promotes good cohesion, chromium improves the tribo-mechanical properties, boron reduces the melting point, silicon increases self-fluxing properties, iron modifies the diffusion rates [6].

WC-based coating is used mainly for marine environment, where sodium is the main content in marine atmosphere (sea salts contain NaCl). [5]

This chapter contains a comprehensive review of the literature with a special reference to hot corrosion of metals and alloys and protective coatings. HVOF process has been described in details.

2.1. Hot Corrosion

Hot corrosion may be defined as an accelerated corrosion, resulting from the presence of salt contaminants such as Na_2SO_4 , NaCl , and V_2O_5 that combine to form molten deposits, which damage the protective surface oxides. Hot corrosion can occur at high temperatures, where the deposit is in the liquid state right from the beginning or the solid deposit turns into liquid during exposure as a result of reaction with the environment. These two types of hot corrosion processes are termed as High Temperature Hot Corrosion (HTHC) or Type I and Low Temperature Hot Corrosion (LTHC) or Type II respectively.[1]

Characteristics of hot corrosion

Hot corrosion is often divided into two forms of attack: Type I (or high-temperature hot corrosion), and Type II (or low-temperature hot corrosion). Various parameters may affect the development of these two forms, including alloy composition and thermomechanical condition, contaminant composition and rate, temperature and temperature cycles, gas composition and velocity, and erosion processes.

Type I hot corrosion (HTHC)

This form of hot corrosion is observed mainly within the temperature range 850-950 °C [3]. HTHC starts with the condensation of fused alkali metal salts on the surface of the component. A cycle of subsequent chemical reactions takes place, initially attacking the protective oxide film and progressing to deplete the chromium element from

the substrate material. With chromium depletion, oxidation of the base material accelerates and porous scale begins to form. The dominant salt in HTHC is Na_2SO_4 due to its high thermodynamic stability. The most significant source of sodium is marine atmosphere (sea salts contain NaCl), but it can also be found in industrial atmospheric pollutants and in volcanic discharges, as well as in the fuel. During combustion, sodium sulfate can form from sodium and sulfur, the latter being present in the fuel. Other impurities either in the fuel or in the air, such as vanadium, phosphorus, lead and chlorides, can combine with sodium sulfate to form a mixture of salts with a lower melting temperature, thus broadening the range of attack. For example, the melting point of Na_2SO_4 (884 °C) can be lowered by the addition of NaCl as an eutectic is formed with a melting point of about 620°C [3].

The presence of sodium chloride removes the incubation period, which otherwise is typical of HTHC [2,3].

HTHC can generally be divided into four progressive stages from initial onset to failure.

1. In stage 1, slight roughening of the surface caused by some growth and localized breakdown of the oxide scale layer is evident. At this stage, neither chromium depletion in the substrate layer nor loss of mechanical integrity are observed.

2. In stage 2, the roughness of the surface is more marked as oxide layer breakdown continues. While chromium depletion commences at this stage, mechanical integrity is still not affected.

3. In stage 3, oxidation of the base material has penetrated to significant depth, with obvious build-up of scale. At this stage, mechanical integrity should be considered as jeopardized and the material removed from service. Progression to stage 4 will accelerate with or without the continued presence of sodium.

4. In stage 4, catastrophic attack occurs. The attack penetrates deeply into the blade while forming a large 'blister' of scale. Failure is likely at this stage due to loss of structural material.

Type II hot corrosion (LTHC)

This form of hot corrosion is observed mainly within the temperature range 650-800 °C [2,3]. LTHC forms typical pitting, resulting from the formation of mixtures of Na₂SO₄ and CoSO₄ with low melting temperatures (the melting temperature of the Na₂SO₄-CoSO₄ eutectic is 540 °C. Similarly, the formation of Na₂SO₄ -NiSO₄ eutectics has been suggested for nickel-based superalloys. Thus, a high partial pressure of SO₃ in the gaseous phase is required for the LTHC reactions to occur, in contrary to HTHC. The localized nature of attack is related to localized failure of the scale as a result of local chloride attack, thermal cycling, or erosion. For example, salt may be trapped locally in crevices produced by scale cracking. Such deposits could be retained and allow local changes in salt composition to occur [3]. As opposed to Type I hot corrosion, in Type II neither incubation period nor microscopic sulfidation and chromium depletion are generally observed.

2.2. Mechanisms of Hot Corrosion

Several mechanisms have been suggested to explain the process of hot corrosion. In this section, only a very brief summary will be presented. The initiation of HTHC is often attributed to failure of the protective oxide layer, which allows the molten salt to access directly the substrate metal. This failure may result from erosion, thermal stresses, erosion-corrosion, chemical reactions, etc. The mechanisms proposed for the HTHC propagation stage are the sulfidation-oxidation mechanism and the salt fluxing mechanisms[2].The salt fluxing mechanism was originally proposed by Goebel and Pettit [14]. According to this model, the protection efficiency of the surface oxide layer

might be lost as a result of fluxing of this layer in the molten salt. The fluxing can be caused either by combination of oxides with O to form anions (i.e. 'basic fluxing') or by decomposition of oxides into the corresponding cations and O activity in the molten salt is markedly lowered, it leads to a much more severe oxidation compared to basic fluxing. As opposed to basic fluxing, acidic fluxing can be self-sustaining, since the displacement of the salt from stoichiometry does not become progressively more difficult as the reaction proceeds. In general, hot corrosion of superalloys with high contents of aluminum and chromium is often reported to occur according to the basic fluxing mechanism. On the other hand, hot corrosion of alloys with high contents of tungsten, molybdenum and vanadium is often reported to follow the acidic fluxing mechanism. Rapp et al. measured the oxide solubilities in molten Na_2SO_4 as a function of the acidity of the salt. Based on these measurements, it was suggested [2] that a negative gradient of the solubility of the protective oxide in the salt film at the oxide/salt interface should lead to oxide dissolution at this interface and to precipitation of a non-protective oxide away from the interface, where the solubility is lower. Fluxing arises in this case only because of the local variation of sodium oxide activity and/or oxygen partial pressure across the salt film; no sulfide-forming reaction is necessary. This mechanism can explain a self-sustaining process of dissolution of the protective oxide to maintain an accelerated corrosion rate [2]. The effect of vanadium on LTHC has been explained by different researchers. Bornstein et al.[28] and Goebel et al.[7] suggested that a self-sustained acidic dissolution of the protective Cr_2O_3 or Al_2O_3 scales could occur when the salt film contains vanadium, because V_2O_5 is a strongly acidic oxide. Zhang and Rapp [2] suggested that every oxide should form an acidic solute with much higher solubility in the presence of vanadate, which should contribute to the more rapid attack of oxides by mixed sulfate-vanadate melts than by a pure sulfate melt. A common model for the occurrence of LTHC was suggested by Luthra [25]. According to this model, LTHC follows two stages:(1)formation of liquid sodium-cobalt sulfate on the surface; and(2) propagation of attack via migration of SO_3 and cobalt inward and outward, respectively, through the liquid salt.

2.3. High Temperature Oxidation Kinetics

Three basic kinetic laws have been used to characterize the oxidation rates of pure metals. It is important to bear in mind that these laws are based on relatively simple oxidation models. Practical oxidation problems usually involve alloys and considerably more complicated oxidation mechanisms and scale properties than considered in these simple analyses.

The parabolic rate law assumes that the diffusion of metal cations or oxygen anions is the rate controlling step and is derived from Fick's first law of diffusion. The concentrations of diffusing species at the oxide-metal and oxide-gas interfaces are assumed to be constant. The diffusivity of the oxide layer is also assumed to be invariant. This assumption implies that the oxide layer has to be uniform, continuous and of the single phase type. Strictly speaking, even for pure metals, this assumption is rarely valid. The rate constant k_p changes with temperature according to an Arrhenius type relationship:

$$x^2 = K_p t + x_0$$

Where: x is the oxide film thickness (or the mass gain due to oxidation, which is proportional to the oxide film thickness), t is time, k_p is the rate constant, directly proportional to the diffusivity of the ionic species that is rate controlling, and x_0 is a constant

The logarithmic rate law is an empirical relationship with no fundamental underlying mechanism. This law is mainly applicable to thin oxide layers formed at relatively low temperatures, and therefore rarely applicable to high temperature engineering problems:

$$x = K_e \log(ct + b)$$

Where: k_e is the rate constant and c and b are constants

The linear rate law is also an empirical relationship that is applicable to the formation and build-up of a non-protective oxide layer.

$$x = K_L t$$

Where: k_L is the rate constant

It is usually expected that the oxidation rate will decrease with time (parabolic behavior), due to an increasing oxide thickness which act as a stronger diffusion barrier with time. In the linear rate law, this effect is not applicable, due to the formation of a highly porous, poorly adherent or cracked non-protective oxide layers. Clearly, the linear rate law is highly undesirable.

Metals with linear oxidation kinetics at a certain temperature have a tendency to undergo so-called catastrophic oxidation (also referred to as breakaway corrosion) at higher temperatures. In this case, a rapid exothermic reaction occurs on the surface, which increases the surface temperature and the reaction rate even further. Metals that may undergo extremely rapid catastrophic oxidation include molybdenum, tungsten, osmium, rhenium and vanadium, associated with volatile oxide formation. In the case of magnesium, ignition of the metal may even occur. The formation of low-melting point oxidation products (eutectics) on the surface has also been associated with catastrophic oxidation. The presence of vanadium and lead oxide contamination in gases deserves special mention, as they pose a risk to inducing extremely high oxidation rates.

2.4. Hot Corrosion of Superalloys

No alloy is immune to hot corrosion attack indefinitely although there are some alloy compositions that require a long initiation times before the hot corrosion process moves from the initiation stage to the propagation stage. Superalloys have been developed for high-temperature applications. However, these alloys may not be able to meet both the high-temperature strength requirements and high-temperature corrosion resistance simultaneously, so may need to be protected against corrosion.[1-3]

The mechanism of Na_2SO_4 induced hot corrosion for nickel base superalloys had been reported by Goebel et al. [7], temperature range 650–1000 °C, temperature range 750–950 °C. The alloys underwent catastrophic corrosion. The accelerated oxidation occurs as a result of the formation of a liquid flux based on Na_2SO_4 , which dissolves the normal protective oxide scales. Catastrophic or self-sustaining rapid oxidation can occur in alloys which contain Mo, W or V because solution of oxides of these elements with Na_2SO_4 decrease the oxide ion activity of the molten salts, producing melts which are acidic fluxes for oxide scales. The evaporation rate of MoO_3 from $\text{Na}_2\text{Mo}-\text{MoO}_3$ melts had been reported to decrease considerably when dissolved in Na_2MoO_4 .

Hot corrosion in sulphate, chloride and vanadate environment of a cast nickel base superalloy had been reported by Deb et al. [8]. Weight gain studies were carried out in air for the uncoated samples and coated with 100% Na_2SO_4 , 75% $\text{Na}_2\text{SO}_4+25\%$ NaCl and 60% $\text{Na}_2\text{SO}_4+30\%$ $\text{NaVO}_3+10\%$ NaCl. The presence of sulphur in the form of sulphates can cause internal sulphidation of the alloy beneath the external oxide layer. Chlorides cause the formation of volatile species, which form voids and pits at grain boundaries, thus forming an easy path for flow of corrodents. The presence of vanadate in conjunction with sulphate and chloride provides additional fluxing action. This destroys the integrity of the alloy and weakens its mechanical properties.

The high-temperature corrosion behaviour of alloy 800 H has been studied by Zhu et al. [9] in an oxidizing and a reducing sulphidising environment at 750 and 850 °C, respectively. When corroded in SO_2-O_2 , the protective chromia scale which developed on the alloy in the early stages cracked and spalled in quite a short time period. This led to the growth of iron and nickel sulfides beneath the chromia layer, causing more chromia spallation.

Malik et al. [10] studied the high-temperature behaviour of commercial alloys, B1900 and IN 100 (Al_2O_3 -formers), Inconel 600, 690, Incoloy 800, IN 738, Nimonic 80A,

100 and 105 (Cr_2O_3 -formers) in the presence of Na_2SO_4 (s) and NaCl (s) separately and in combination at 850 and 1000 °C in air. They concluded that the Cr_2O_3 formers get attacked more aggressively by NaCl (s) than Na_2SO_4 (s). Al_2O_3 formers and to some extent NiO -formers are more resistant to NaCl attack than Cr_2O_3 formers. While Na_2SO_4 induced corrosion proceeds by fluxing and sulphidation reactions, the NaCl induced corrosion follows a reaction path of fluxing, chloridation and oxidation. The Na_2SO_4 - NaCl induced corrosion involves combination of reactions occurring in the presence Na_2SO_4 and NaCl separately.

Gurrappa [11], during hot corrosion studies on CM 247 LC superalloy in Na_2SO_4 and Na_2SO_4 + NaCl mixtures at 900 °C, observed that bare CM 247 LC got severely corroded in just 4 h, while it was completely consumed in 70 H when tested in 90% Na_2SO_4 +10% NaCl at 900 °C. The results showed that a chloride containing melt is more corrosive than pure sodium sulphate.

Johnson et al. pointed out that the presence of NaCl in the mixtures of $\text{NaCl}/\text{Na}_2\text{SO}_4$ could initiate attack in high chromium content alloys. The addition of 10% NaCl in Na_2SO_4 coatings can easily cause the cracking of protective Cr_2O_3 layers and increase the amount of sulphur incorporated into the substrate, accelerating the corrosion of alloys. Even if the oxidation reaction takes place first, localized chemical dissolution of oxides into the molten chloride occurs. Thus, in the initial stage oxide scales on the alloy surface could be degraded by molten NaCl . NaCl was responsible for the subscale attack of 310 SS, the depth of internal attack increased with increasing NaCl content in salt mixtures.[12]

Chang- Cheng Tsaur C.rock, Chaur-Jeng Wang and Yung-Hua Su (2004) studied the high temperature corrosion behaviour of '310 stainless' steel at air 750 C in air with 2 mg/cm² mixtures of various $\text{NaCl}/\text{Na}_2\text{SO}_4$ ratios. The corrosion behavior and morphological development were investigated by weight gain kinetics, metallographs,

depth of attack, metal losses and X-ray analysis. The results show that weight gain kinetics in simple oxidation reveals a steady-state parabolic rate law after 3h, while the kinetics with salt deposits display multi-stage growth rates. NaCl is the main corrosive specie in high temperature corrosion involving mixtures of NaCl/Na₂SO₄ and is responsible for the formation of internal attack. The most severe corrosion takes place with the 75% NaCl mixtures. Uniform internal attack is the typical morphology of NaCl induced hot corrosion, while the extent of intergranular attack is more pronounced as the content of Na₂SO₄ in the mixture is increased.[13].

2.5. Protective coating

The coating can be defined as a layer of material formed naturally or synthetically or deposited artificially on the surface of an object made of another material, with the aim of obtaining required technical or decorative properties. Coating provides a way of extending the limits of use of materials at the upper end of their performance capabilities, by allowing the mechanical properties of the substrate materials to be maintained, while protecting them against wear or corrosion [1,8].

Coatings are frequently applied to the surface of materials to serve one or more of the following purposes:

- 1 To protect the surface from the environment that may produce corrosion or other deteriorative reactions.
- 2 To improve the surface appearance.

There are many coating deposition techniques available, and choosing the best process depends on the functional requirements, (size, shape, and metallurgy of the substrate), adaptability of the coating material to the technique intended, level of adhesion required, and availability and cost of the equipment.[14]

2.5.1 Considerations in Coating Selection

The specifier should consider following aspects of the proposed coating job in order to select the most appropriate coating system.

a. Limits on surface preparation. Coating selection may be limited by the degree or type of surface preparation that can be achieved on a particular structure or structural component. Because of physical configuration or proximity to sensitive equipment or machinery, it may not always be possible to abrasive-blast a steel substrate. In some cases, it may be necessary to remove the old coating by means other than abrasive-blasting, such as power tools, water jetting, or chemical strippers. In the case of thermal spray coatings, a high degree of surface preparation is essential. This kind of preparation can only be achieved by abrasive blasting with a good quality, properly sized angular blast media. Thermal spray should never be selected for jobs where it is not possible to provide the highest quality surface preparation.

b. Ease of application. Coating selection may be limited by the ability of the applicator to access the surfaces to be coated. This usually is the result of the physical configuration or design of the structure. Items of limited access such as back-to-back angles, cavities, and crevices may be difficult if not impossible to coat. Thermal spray coatings perform best when sprayed in a direction normal to the surface and within a particular range of standoff distances from the substrate. Application at an angle of less than 45 deg to the vertical is not recommended. Maximum and minimum standoff distances depend on the material being applied, the manufacturer, and the type of thermal spray equipment.

c. Field conditions. The conditions under which the coating work will be performed are another important consideration in coating selection. Certain atmospheric conditions, including high humidity and condensation, precipitation, high winds, and extreme cold or heat, place severe limitations on any type of coating work. (1) Moisture on the surface should always be avoided to the greatest extent possible. Thermal spray metal coatings should never be applied if moisture is present on the

surface. (2) High winds may affect the types of surface preparation and coating application methods that are practical for a given job. This problem can be avoided by using methods other than open abrasive blasting and spray application of paints.

(3) There are generally no upper or lower ambient or surface temperature limits on the application of thermal spray coatings, although there are practical limits at which workers can properly perform their tasks. In thermal spray, the steel substrate is generally preheated to well above ambient temperatures to drive off any latent moisture and to prevent condensation from forming on the surface. In addition, any ill effects that a cold substrate might have are ameliorated.

d. Maintainability. The future maintainability of the coating system should be considered by the specifier. Some protective coatings are easier to maintain than are others. Thermal spray coatings are difficult to repair. Because of the difficulty affecting appropriate repairs, the thermal spray coating systems, are generally kept in service until total recoating is needed.

e. Extremes of pH. Extremes of pH, such as strongly acidic or alkaline environments can greatly affect coating performance. The coating must be relatively impermeable to prevent migration of the acidic or alkaline aqueous media to the substrate, and the coating material itself must be resistant to chemical attack. Thermal spray coatings of aluminum, zinc, and their alloys may perform poorly in both high and low pH environments. Both metals show increased solubility as pH increases or decreases from the neutral pH of 7. Thermal spray aluminum and zinc may be used in acidic or alkaline environments provided that they are sealed and topcoated with vinyl or epoxy coatings. Unsealed zinc thermal spray coatings are suitable for pHs of 6 to 12 and aluminum thermal spray coatings for pHs of 4 to 8.5. Thermal spray coatings containing zinc or aluminum should not be used in chemical environments where they may be exposed to strong acids such as battery acids. Organic coatings and linings, as well as special inorganic building materials, should be used in highly alkaline or acidic environments.

f. **Cost.** Coating systems are cost effective only to the extent that they will provide the requisite corrosion protection. Cost should be considered only after the identification of coatings that will perform in the exposure environment. Given that a number of coating systems may perform for a given application, the next consideration is the cost of the coating job. Ideally, protective coating systems will always be selected based on life-cycle cost rather than simple installed cost. However, given the realities of budgets, this approach is not always practical. Therefore, coating systems are sometimes selected on the basis of first or installed cost. Because thermal spray coating systems are almost always more expensive to install than paint systems for a given application, they are often passed over, when, in fact, they can have significantly lower life-cycle costs than paint systems. [15,18]

2.6. Thermal Spray Coating

Thermal spraying is a process by which finely divided metallic or nonmetallic materials are deposited in a molten or semimolten condition on a prepared substrate to form a sprayed deposit. Thermal spray processes include combustion powder flame spray, combustion wire flame spray, wire arc spray, plasma spray, and high velocity oxyfuel (HVOF) spray. Thermal spraying that uses the heat from a chemical reaction is known as combustion gas spraying, or flame spraying. Any material that does not sublime (i.e., does not transform directly from a solid to gas) and has a melting temperature of less than 5000 °F may be flame sprayed. Materials that are applied by flame spray include metals or alloys in the form of wire, cord, or powder; ceramics as powder, cord, or rod; and polymers as powder. Combustion wire flame spray feedstock material is mechanically drawn by drive rollers into the rear of the gun. The feedstock proceeds through a nozzle where it is melted in a coaxial flame of burning gas. One of the following gases may be combined with oxygen for use in flame spraying: acetylene, methylacetylenepropadiene stabilized (MPS), propane, hydrogen, or natural gas. Acetylene is the gas most widely used because of higher flame temperature. The fuel gas flame is used for melting only—not for propelling or

conveying the material. To accomplish spraying, the flame is surrounded with a stream of compressed gas— usually air—to atomize the molten material and to propel it onto the substrate. The combustion powder flame spray process is similar to the wire process but the powder feedstock is stored in a hopper that can either be integral to the gun or externally connected to the gun. A carrier gas is used to convey the powder into the oxygen fuel gas stream where the powder is melted and carried by the flame onto the substrate. In the wire arc process, two consumable wire electrodes, which are at first isolated from each other, automatically advance to meet at a point in the atomizing gas stream. An electrical potential difference of 18 to 40 volts, applied across the wires, initiates an arc that melts the tip of the wire electrodes. An atomizing gas, usually compressed air, is directed across the arc zone, shearing off the molten droplets that form the atomized spray. Plasma spray technology uses a plasma-forming gas (usually either argon or nitrogen) as both the heat source and the propelling agent for the coating. A high-voltage arc (up to 80 kW) is struck between the anode and cathode within a specially designed spray gun. This energy excites the plasma gas into a state of ionization. The excited gas is forced through a convergent/divergent nozzle. Upon exiting the nozzle, the gas returns to its natural state, liberating extreme heat. Powder spray material is injected in the hot plasma stream, in which it is melted and projected at high velocity onto a prepared substrate. The resulting coatings are generally dense and strongly bonded with high integrity.[16,18]

2.6.1 HVOF Spraying

The HVOF process efficiently uses high kinetic energy and controlled heat output to produce dense, very-low-porosity coatings that exhibit high bond strength. The HVOF gun consists of a nozzle to mix the combustion gases, an air-cooled combustion chamber, and an external nozzle (air cap). The process gases enter through several

coaxial annular openings. A central flow of powder and carrier gas is surrounded by air, fuel, oxygen, and the remaining process in air. This focuses the spray stream and prevents the powder from contacting the gun walls. The oxygen and fuel burn as they enter the rear portion of the combustion chamber. Most of the process air is used to cool the combustion chamber. As it enters, the process gas forms a thin boundary layer that minimizes the contact of the flame with the walls of the air cap and helps to reduce the quantity of heat transferred to the air cap. Hot gases with a combustion temperature of up to 3300 °C exit through a converging nozzle with a gas velocity that can approach 4500 ft/sec (Metco 1996). For the application of polymeric or thermal spray coatings the surface must be cleaned and have a suitable profile that will enhance the coating adhesion. Cleaning procedures are designed to remove specific types of contaminants without changing the physical or chemical properties of the substrate surface. Cleaning can be done with solvents that dissolve the contaminants. A rough profile has a greater surface area, which increases bonding capability. Surfaces can be roughened by machining or grit blasting. Thermal spray coatings are generally limited in the thickness of material that can be deposited. This limit can be as low as 0.030 in. for plasma spray and HVOF coating processes. However, in some cases 1 in. thick coatings have been applied. Due to thickness limitations, deep cavitation damage would have to be repaired by welding, but thermal spray coatings could be applied to the welded surface to provide additional protection to the component. Thermal spray coatings could also be applied directly to properly cleaned and roughened surfaces that do not require weld repair. It is anticipated that once a sprayed coating is applied, this coating will prevent damage to the underlying base metal. Because the sprayed coating becomes the active surface, future repairs of the affected area can be made using thermal spray coatings deposited by the HVOF process rather than by weld repair of the substrate, which costs approximately three times as much as flame spraying [12,14].

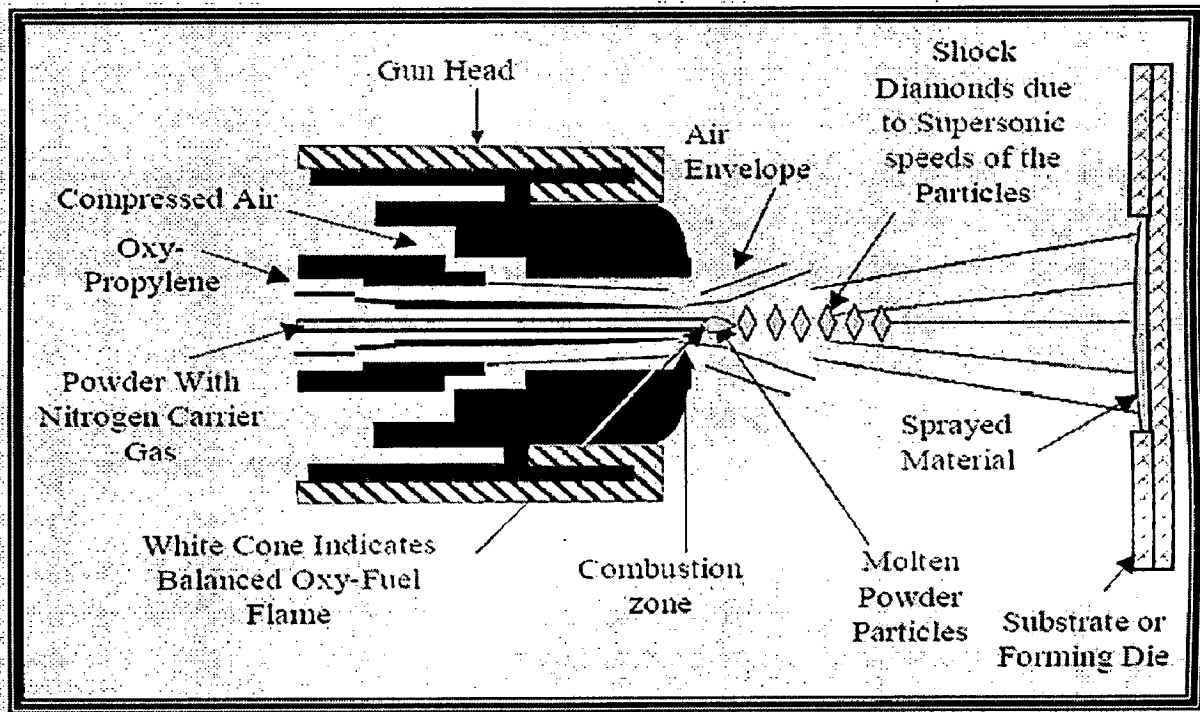


Fig 2.1 Schematic cross-section of Diamond Jet spray gun and key parameters relating to the HVOF coating process.

<i>Process Characteristics</i>	
Jet Temperature	Generally >2,500 °C
Jet Speed	Typically >1,000 m/s
Gas Flow Rate	400-1,100 slm
Particle Speed	200-1,000 m/s
Powder Feed Rate	2-50 g/min

Equipment for the HVOF process consists of a controller for the gases, fuel, and powder, a powder feeder, and a torch.

The benefits of HVOF over weld overlays are as follows:

- No preheating
- No dilution
- No distortion
- Reduced coating time, typically only 20 percent of weld time
- Removal of post-coating machining
- Reduced reject rates (fewer discontinuity types)

The benefits of HVOF over plasma and arc spraying are as follows:

- Lower porosity - no post-coating sealant or fusion
- Higher bond and cohesive strength
- Lower oxide content
- Better retention/control over particle chemistry and phases
- Thicker coatings

Herman et al. [19] reported that HVOF spraying is able to make denser and less oxidized coatings compared with other methods, such as plasma spraying. Furthermore, this spraying system enables metals and alloys with high melting point up to about 2000 °C to be deposited on the target surface. These features are suitable for a deposition of corrosion resistant coatings. Fig. 2.2 indicates the characteristics of HVOF coatings compared with those produced using the standard plasma spraying process [1]

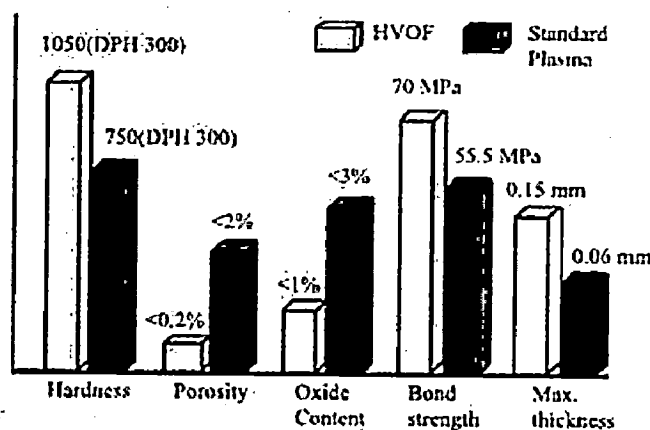


Fig 2.2 Characteristics of HVOF and standard plasma sprayed coatings

Scope

Hot corrosion has been identified as a serious problem in high temperature applications such as in boilers, gas turbines, waste incinerators, diesel engines, coal gasification plants, chemical plants and other energy systems. It is basically induced by impurities such as Na, V, S etc. present in the coal or in the fuel oil used for combustion in mentioned applications. In some situations these impurities may be inhaled from the working environment for instance, NaCl in marine atmospheres. There is a general agreement that condensed alkali metal salts notably Na_2SO_4 are prerequisite to hot corrosion. Due to high cost of removing these impurities, the use of these low grade fuels is usually justified.

For the reason that hot corrosion of components in aforesaid high temperature environments is inevitable, the phenomenon has maintained its relevance from last more than 60 years. Hot corrosion often increases the corrosion loss of heat resisting alloys by over hundred times, in comparison to that incurred by simple oxidation.

Power plants are one of the major industries suffering from severe corrosion problems resulting in the substantial losses. For instance, steam temperature of boilers is limited by corrosion and creep resistance of boiler components, which affects the thermal efficiency of boilers. Consequently, the thermal efficiency decreases and the electricity production is reduced.

Objective

The present work is a comparative study of HVOF sprayed WC-NiCrFeSiB coating on a Ni-based superalloy (SN 75) and Fe-based superalloy (800H) in the different environments, such as simple oxidation (in presence of air only) and a molten salt environment (of 75% Na_2SO_4 +25%NaCl) at 800 °C under cyclic conditions. The salt

mixture consisting of 75% Na_2SO_4 -25% NaCl constitutes an eutectic with a low melting point of 750 °C and provides a very aggressive environment for accelerated testing under simulated laboratory conditions.

Oxidation studies were conducted on uncoated superalloys as well. Oxidation time of 50 hr is considered adequate to allow for steady state oxidation. Experiments were proposed to be conducted in SiC tube furnace. The thermogravimetric technique was used to establish the kinetics of corrosion. X-ray diffraction, scanning electron microscopy techniques were used to analyse the corrosion products.

The temperature of study was deliberately kept high (800 °C) as this will also take into consideration the overheating effect in case of boilers which has been identified as the major cause of failure. Moreover at 800 °C the rate of hot corrosion has been reported to be severest. It was proposed to conduct the experiment under cyclic conditions as these conditions constitute more severe condition and realistic approach towards solving the problem of metal corrosion in actual applications, where conditions are more or less cyclic rather than isothermal. Fewer studies were reported on hot corrosion of superalloys under cyclic conditions.

4.1 Substrate Material

The substrate material selected for the study was Fe based superalloy (Superfer 800H) and Ni based superalloy (Sn75), which was procured from Mishra Dhanu Nigham Limited, Hyderabad (India) in the rolled sheet form. The chemical composition of the substrate material is

Table 4.1

Nominal chemical composition of the substrate materials

Alloy Midhani Grade (Similar Grade)	Chemical Composition (wt %)							
	Fe	Ni	Cr	Ti	Al	Mn	Si	C
Superni 75	3.0	77.1	19.5	0.3	-	-	-	0.1
Superfer 800H	43.8	32.0	21.0	0.3	0.3	1.5	1.0	0.1

4.2 Sample Preparation

The specimens with dimensions of approximately 20 mm X 15 mm X 5 mm were cut from the alloy sheets. They were polished on emery papers of grade 1/0, 2/0, 3/0 and 4/0 respectively. Polishing was done on a soft polishing wheel with fine grit size alumina powder slurry. After polishing the specimens were rinsed with water and dried. They were reexamined under optical microscope to check their roughness.

Saturated salt solutions were prepared at room temperature. Hot and saturated mixture of 75% Na₂SO₄+25%NaCl was sprayed over the specimen heated at 250 °C. The specimens were dried in electric oven at 100 °C for small interval of time.

4.3 Coating Formulation

HVOF coating used here is WC-NiCrFeSiB .

Table 4.2

Chemical composition of WC-NiCrFeSiB :

W	28.3%
CO	4.2%
Cr	9.9%
Ni	46.5%
B	2.0%
Si	2.9%
Fe	2.7%
C	2.3%
Others	< 1.2%

Particle Size is -45 to +15 micron

Samples were grit-blasted before the HVOF spraying. All the process parameters, including the spray distance, were kept constant throughout the coating process with an Oxygen flow rate 250 LPM ,Fuel (LPG) flow rate 70 LPM, Air flow rate 6200 LPM, Spray distance 200 mm, Powder feed rate 30 g/min, Particle size -45+15 μ m. 100 μ m thick coating was deposited with a collaboration of Metallizing Equipment Co. Jodhpur (India) on a commercial HIPOJET-2100 (MEC Jodhpur, India) apparatus operating with oxygen and LPG as the fuel gases. The substrates were cooled with compressed air jets during and after spraying.

4.4 Molten Salt Corrosion Test

There is no standard procedure that has yet been evolved for carrying out cyclic oxidation tests. Different investigators have employed different holding times at different temperatures. and rate of heating and cooling also not been generally

specified. In the present study cyclic oxidation tests were used to compare the extent of oxide spallation of the different specimens.

These studies were performed in molten salt ($\text{Na}_2\text{SO}_4\text{-NaCl}$) for 50 cycles. Each cycle consisted of 1 h heating at 800 °C in Silicon Carbide tube furnace followed by 20 min cooling at room temperature. The specimens were kept in alumina boats and then the boats were inserted in the furnace. The aim of cyclic hot corrosion is to create accelerated conditions for testing. The studies were performed for uncoated as well as coated specimens for the purpose of comparison. The specimens were mirror polished down to 1 μm alumina wheel cloth polishing before corrosion run. The coating of uniform thickness with 3–5 mg/cm^2 of $\text{Na}_2\text{SO}_4\text{-NaCl}$ was applied with camel hairbrush on the preheated sample (250 °C). The weight change measurements were taken at the end of each cycle with help of Electronic Balance machine Model 06120 (Contech) with a sensitivity of 1 mg. The spalled scale was also included at the time of measurements of weight change to determine total rate of corrosion. Efforts were made to formulate the kinetics of corrosion. The samples after oxidation were analyzed by XRD & SEM.

Visual Observation

Visual examinations of the exposed samples were made for their color, luster adherence, and spalling tendency. Samples were visually examined for changes in surface scales.

X-ray Diffraction

This was carried out for phase identification of the oxidation products. This XRD analysis of the oxidized specimens was carried out with Burker AXS D-8 Advanced Diffractometer (Germany). The other specifications were:

Target	Cu
Filter	Ni

Current	20/15mA
Voltage	35 kV
Angle range	20°-110°
Chart speed	1cm/min
Gm sped	2°/min
Range	2KC/s
Wavelength	1.54 Å

Diffraction patterns were analyzed by adopting the following procedure:

1. 'd' values were obtained for all the discernable reflections/peaks in the usual manner.
2. Assuming the height of the most prominent peak reflection to be 100% the relative intensities of all peaks/ reflections were determined.
3. Above data was compared with ASTM data following standard procedures and phase identification was carried out.

Scanning Electron Microscopy

Surface morphology of the specimen was examined by taking SEM micrographs using Scanning Electron microscope [JEOL (JSM-5800)]. A number of photographs were taken, mostly at 150 X, 1K X, 2K X, 3K X and 5K X for each of the samples.

4.5 Sources of Error

- Improper accuracy of the temperature controller of the furnace.
- Non uniformity of temperature along the length of the tube of furnace.
- Frequent power failures during the heating cycles.
- Non-Uniformity of the coating.

4.6 Precautions

- Specimen should be polished on the emery papers so that uniformity of the coating is maintained, excessive polishing may erode off the coatings too much.
- Furnace should be calibrated before using.
- Only one specimen should be kept in a furnace at a time.
- The specimen along with the boats should be properly dried before keeping in the furnace.

5.1 UNCOATED SUPERALLOYS

5.1.1 Hot Corrosion Study

5.1.1.1 Visual Observation

A brownish grey scale appeared on the surface of uncoated superalloys superni 75 and superfer 800 H after salt oxidation for 50 cycles at 800 °C, during the initial cycles which turned to dark grey after third cycle. The cracks were developed in the scale and spalling was observed during the course of study. Initially, the spalling was confined to edges and corners, but after 12th cycle, spalling also occurred from the surface of the uncoated superalloy. The spalling tendency of the scale formed on uncoated superalloys can also be seen in SEM (Fig5.5).

Colour of oxide scale formed on the uncoated superalloys superni 75 and superfer 800H after air oxidation for 50 cycles at 800 °C was dark grey, in general with some brownish spots. In case of Superfer 800H, greenish tinges were also observed (from the 10 th cycle onwards) in the scale in early cycles of study. A bluish tinge was observed in Superni 75 from 12th cycle onwards and at the 15th cycle, the sample turned completely light blue. Lustrous scales were formed upto mid cycles of the study, which eventually went on becoming dull with increasing number of cycle.

5.1.1.2 Oxidation Kinetics

The weight gain/unit area results for the superalloy substrates without WC-NiCrFeSiB coating exposed to the 75%Na₂SO₄+25%NaCl salt mixture and air oxidation at 800 °C for 50 cycles are shown in Fig5.1. After 30th cycle oxidation rate has become nearly constant. Fe-based uncoated superalloy Superfer 800H shows the maximum weight gain, whereas bare Superni 75 shows the minimum in both the environments (with or

without salt). The weight gain of Superni 75 after 50 cycles is nearly one-third of that of Superfer 800H.

During the course of the study, it was observed that the uncoated Superfer 800H superalloy underwent much spalling as well as sputtering, whereas uncoated Superni 75 showed less

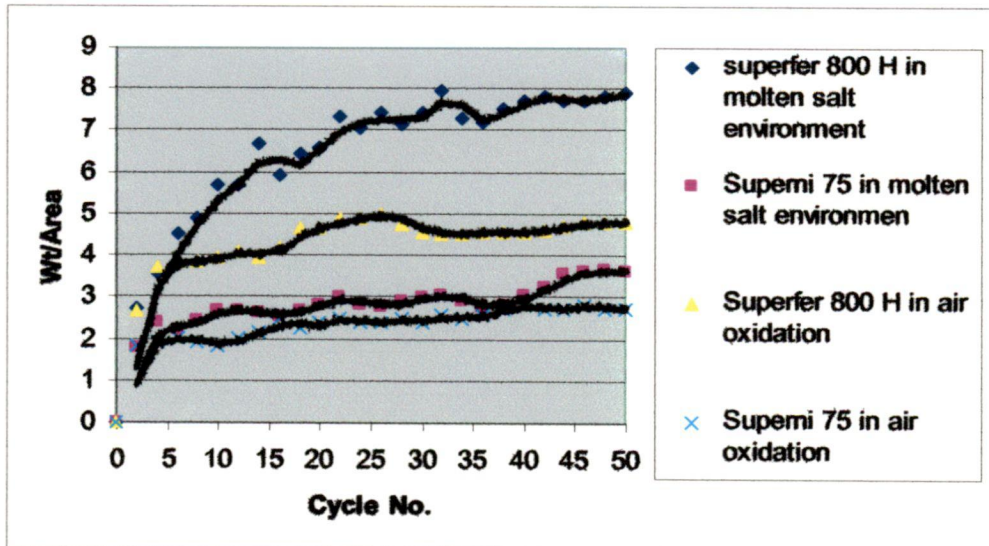


Fig 5.1 Study of Corrosion Kinetics of Bare Superalloys

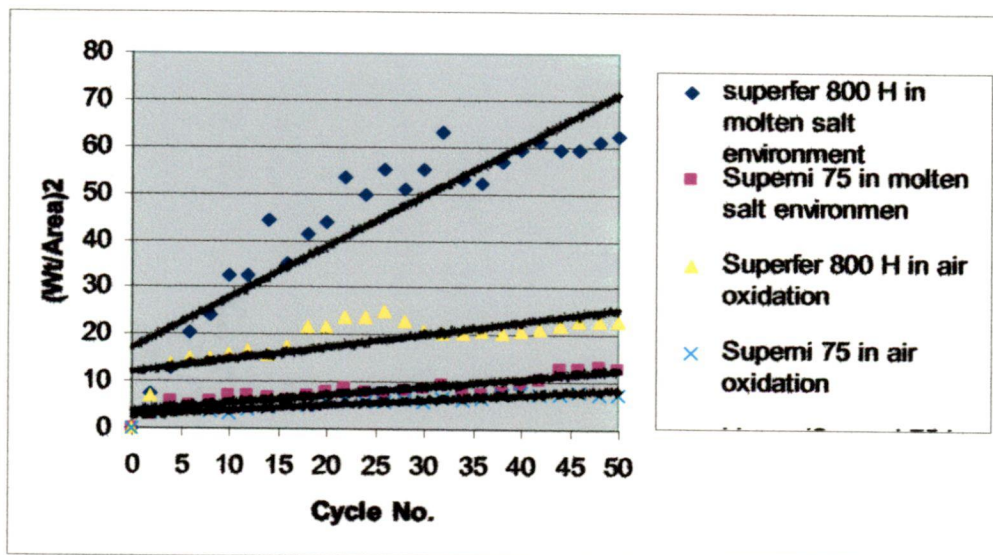


Fig 5.2 $(\text{Weight gain} / \text{area})^2$ vs number of cycles plot for Bare Superalloys

Table 5.1 Values of Parabolic rate constant K_p for bare superalloys

Sample	K_p ($\text{g}^2\text{cm}^{-4}\text{sec}^{-1}$)
Superfer 800 H in presence of molten salt	98.6×10^{-10}
Superni 75 in presence of molten salt	71.2×10^{-10}
Superfer 800 H in presence of simple air oxidation environment	36.0×10^{-10}
Superni 75 in presence of simple air oxidation environment	22.5×10^{-10}

spalling/sputtering. Sputtering of uncoated Superfer 800H occurred continuously during the period of cooling or even while keeping the sample inside the furnace, which might have affected the weight gained by the bare superalloy and the actual weight gain might be more than what was observed. Cracks appeared in the scales of uncoated superalloys and are clearly the formation of a unprotective scale on an alloy by selective oxidation necessarily depletes the scale-forming element from the underlying alloy. Particularly important among these conditions are temperature cycling, which causes loss of protective scale by spallation. The cause for spallation is stress, generated from thermal expansion mismatch between the scale and alloy (thermal stresses) which may be superposed on stresses generated by scale growth (growth stresses). In fig 5.2 superfer 800 H after hot corrosion shows deviation from the parabolic rate law, whereas superni 75 follows the parabolic rate law.

5.1.2 Characterization of Corrosion Products

5.1.2.1 X-ray Diffraction Analysis of Scales

The XRD profiles for the scale of bare superalloys after hot corrosion in 75% Na_2SO_4 -25% NaCl environment for 50 cycles at 800 °C are shown in Fig. 5.3. The major and minor phases detected at the surface of the specimens are shown in the XRD graph. The existence of MnO_2 phase on the surface of hot corroded Superni 75 and Superfer 800 H respectively, indicates the diffusion of Mn from the substrate during hot corrosion of the specimens at temperature about 800 °C.

The XRD profiles for the scale of bare superalloys in the air oxidation is shown in fig. 5.4 It shows the formation the NiCr_2O_3 , Fe_2O_3 and Cr_2O_3 as the major phase.

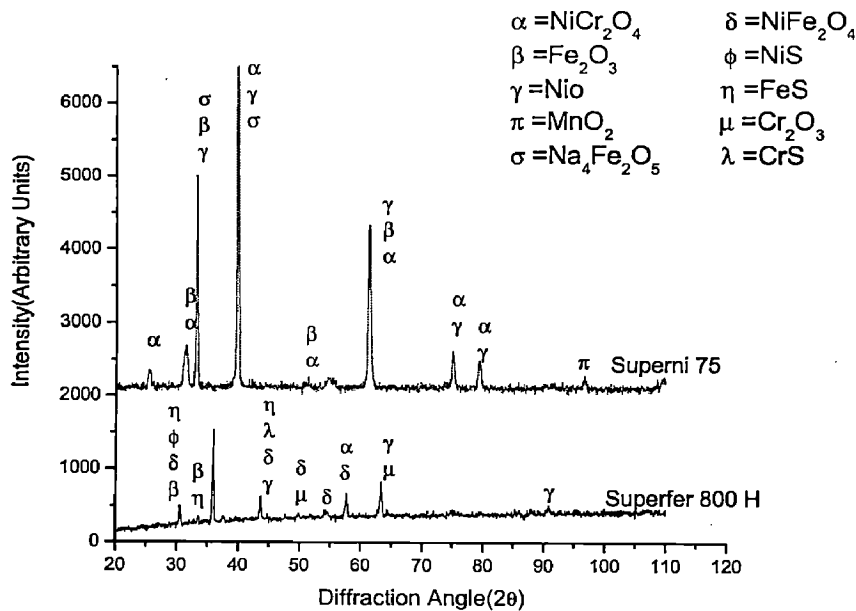


Fig 5.3 XRD of bare superalloys in presence of molten salt environment

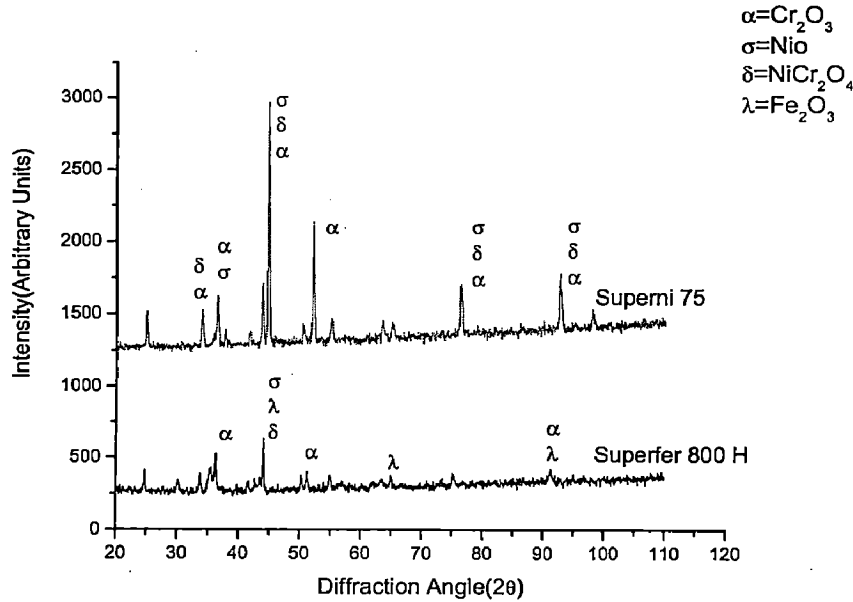


Fig 5.4 XRD of bare superalloys in presence of simple air oxidation environment

5.1.2.2 SEM Analysis

SEM micrographs of the uncoated superfer 800 H, shows surface morphology after cyclic hot corrosion for 50 cycles at 800 °C (Fig.5.5). The scale formed on uncoated Superfer 800H is found to be more fragile in nature. The micrographs of all the corroded uncoated superalloys clearly indicate the presence of cracks as well as spalled region. At higher magnification these cracks and spalled regions are clearly seen in fig5.5.

In the hot corrosion attack by 75% Na_2SO_4 -25% NaCl corrodent, NaCl reacts with the oxides releasing chlorine, which in turn reacts with the oxides to form volatile chlorides. The volatile species thus formed tend to diffuse out of the grain boundaries to the surface and in doing so numerous pits and voids are generated at the grain boundaries (Fig.5.5), which can be seen clearly. For the 75% Na_2SO_4 +25% NaCl coated samples, indicates the formation of continuous and regular scale containing of fine grains.

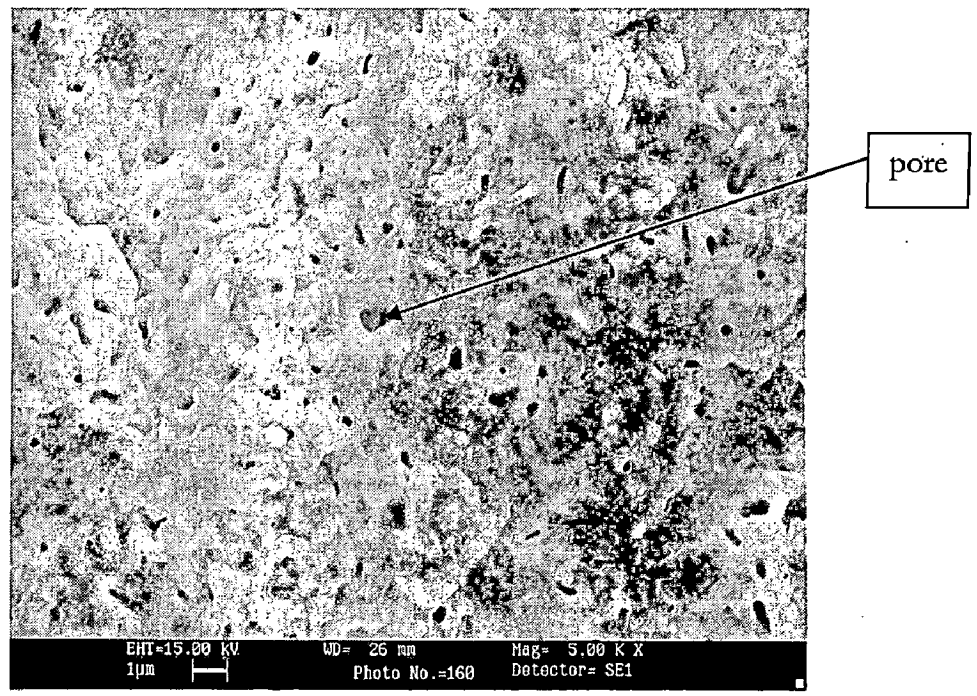
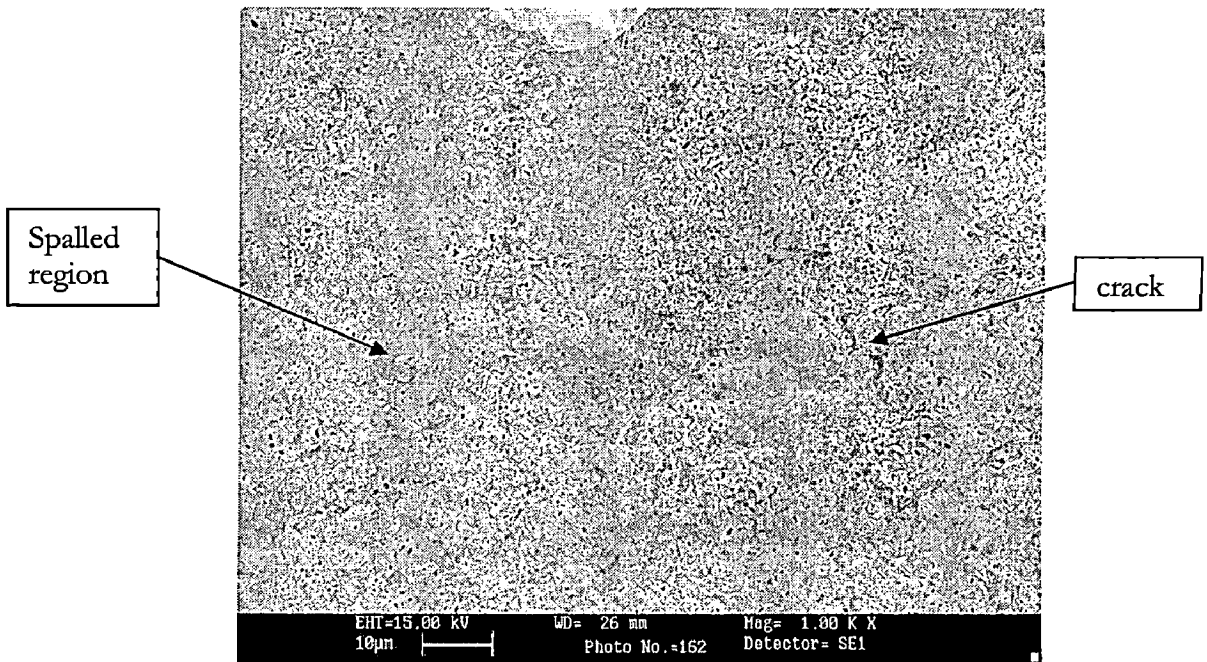


Fig 5.5 SEM of uncoated Superfer 800 H after corrosion in molten salt environment of $75\%Na_2SO_4 + 25\%NaCl$

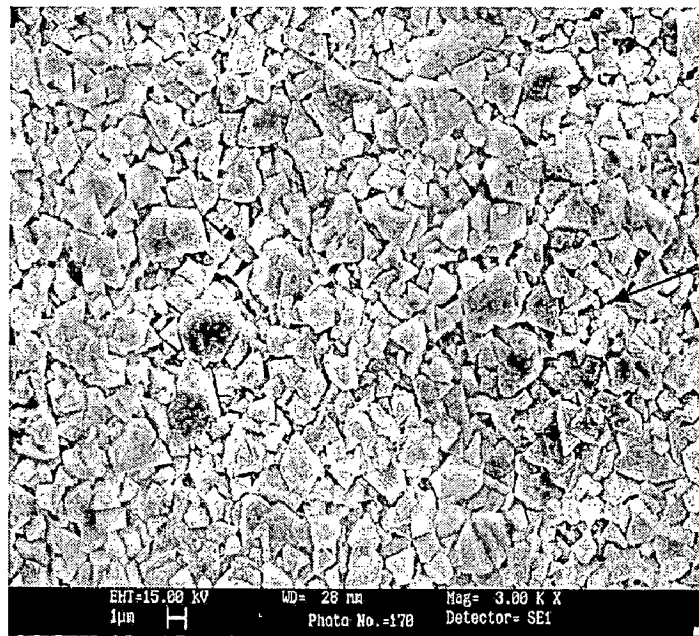
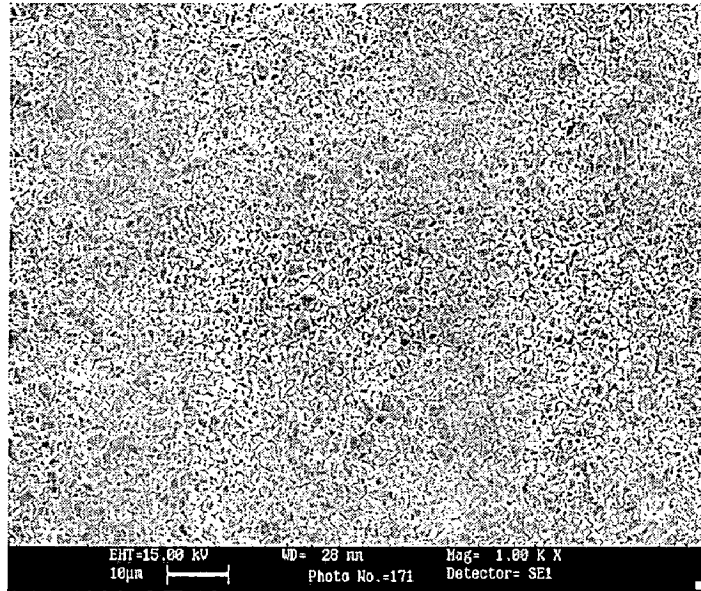


Fig5.6 SEM of uncoated Superni 75 after corrosion in molten salt environment of $75\%Na_2SO_4 + 25\%NaCl$

5.1.2.3 Cross-sectional analysis of the oxide scales

BSE images of Uncoated superalloys after corrosion in molten salt environment of 75%Na₂SO₄ + 25%NaCl are shown in fig below.

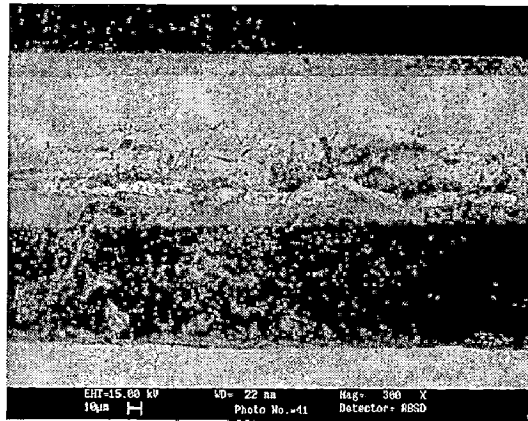


Fig 5.7 BSE images of Uncoated Superfer 800 H after corrosion in molten salt environment of 75%Na₂SO₄ + 25%NaCl

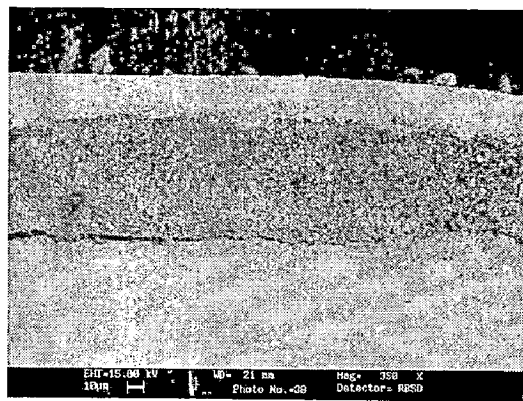


Fig 5.8 BSE images of Uncoated Superni 75 after corrosion in molten salt environment of 75%Na₂SO₄ + 25%NaCl

5.2 COATED SUPERALLOYS

5.2.1 Hot Corrosion Study

5.2.1.1 Visual Observations

The WC-NiCrFeSiB coated Superfer 800H showed minor cracks at the edges and corners, and spalling from these regions occurred from 12th cycle. The colour of the scale which was dark grey during the earlier cycles turned to blackish green with the progress of the study. In the case of coated Superni 75, a blackish grey scale was formed after first cycle which gradually turned to dark black during next few cycles. Subsequently after 15th cycle, a very shining silver grey scale appeared which lasted up to the end of study. The scale was smooth and intact, and spalling of the scales was negligible. Mostly marginal spalling of the coatings was observed near and/ or the edges.

5.2.1.2 Corrosion Kinetics

The weight gain/unit area results for the two superalloy substrates with WC-NiCrFeSiB coating exposed to the 75% Na₂SO₄-25%NaCl salt mixture at 800 °C for 50 cycles are shown in Fig5.9. It can be inferred from the above figures that the oxidation rate can be divided into two stages:

1. The transient oxidation stage which shows initial rapid oxidation rate
2. The steady state oxidation stage.

The coated superalloys in all cases show a much lower weight gain(fig5.9) than the uncoated specimens (fig5.1) in the given molten salt environment. The WC-NiCrFeSiB coating provides the maximum hot corrosion resistance to Superni 75 and has been found successful in reducing the weight gain by 80% of that gained without a coating. Further, the coated superalloys in all cases show an almost similar weight gain. Fig. 6.1 shows the cumulative weight gain/unit area in all the cases of uncoated/coated superalloys.

A rust-colored compact and dense continuous scale was found to be formed on the hot corroded WC-NiCrFeSiB coated superalloys and no spallation or peeling off of the scale was noticed. It is observed from the graph that all the coatings follow a nearly parabolic rate law (Fig 5.10) and thus they have a tendency to act like diffusion barriers to the corroding species.

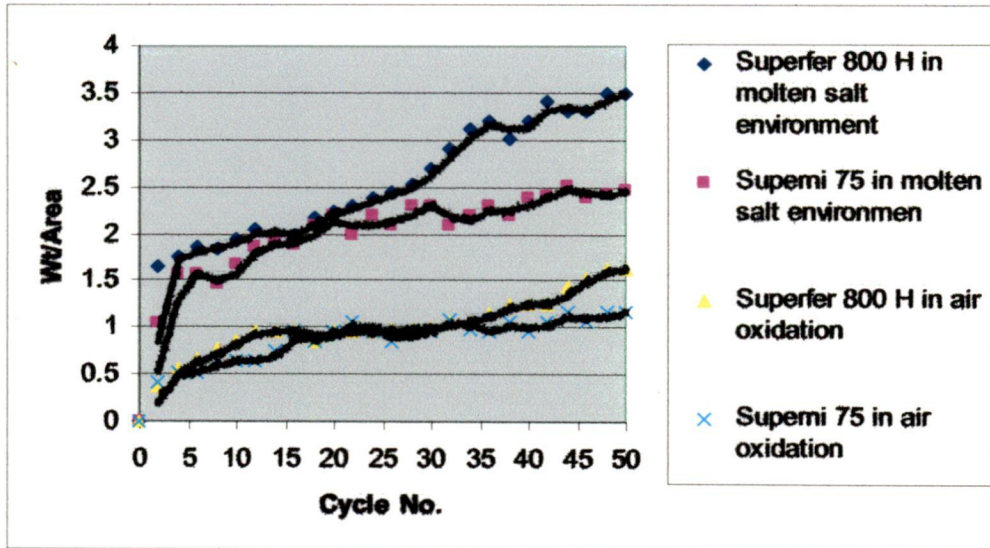


Fig 5.9 Study of Corrosion Kinetics of coated superalloys

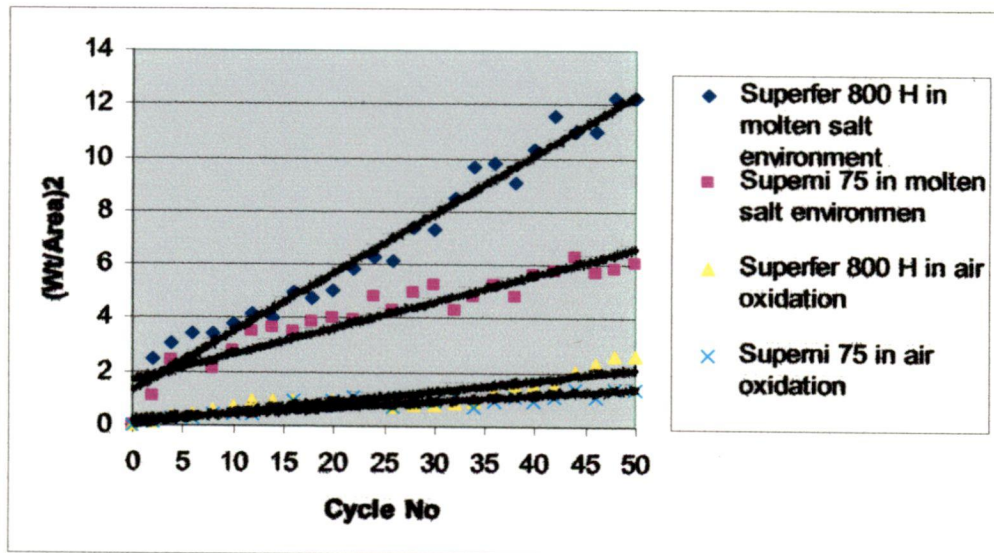


Fig 5.10 $(\text{Weight gain} / \text{area})^2$ vs number of cycles plot for Coated Superalloys

Table 5.2 Values of Parabolic rate constant K_p for WC-NiCrFeSiB coated superalloys

Sample	K_p ($\text{g}^2\text{cm}^{-4}\text{sec}^{-1}$)
Superfer 800 H in presence of molten salt	11.6×10^{-10}
Superni 75 in presence of molten salt	9.1×10^{-10}
Superfer 800 H in presence of simple air oxidation environment	3.0×10^{-10}
Superni 75 in presence of simple air oxidation environment	2.5×10^{-10}

5.2.2 Characterization of Corrosion Products

5.2.2.1 X-ray Diffraction Analysis

The XRD profiles for HVOF coated superalloys in presence of salt after hot corrosion in 75% Na_2SO_4 -25% NaCl environment for 50 cycles at 800 °C are shown in Fig.5.11. The major and minor phases detected at the surface of the specimens with the XRD analysis are shown in fig. The main phases identified for corroded coated Superalloys in presence of salt are Cr_2O_3 , $\text{FeO} \cdot \text{Fe}_2\text{O}_3$, CoCr_2O_4 , $\text{Na}_4\text{Fe}_2\text{O}_5$, Co_3BO_5 , NiCr_2O_4 , NiFe_2O_5 and NiO . The hot corroded WC-NiCrFeSi coated Superni 75 and Superfer 800H indicate the formation of similar phases.

The XRD profiles for HVOF coated superalloys in presence of simple air oxidation environment for 50 cycles at 800 °C are shown in Fig.5.12. The major and minor phases detected at the surface of the specimens with the XRD analysis are shown in fig. The main phases identified for corroded coated Superalloys in presence of air are WC, Ni, CoCrO_4 , NiCr_2O_4 , FeNi_3 and Cr_2O_3 . The hot corroded WC-NiCrFeSi coated Superni 75 and Superfer 800 H indicate the formation of similar phases.

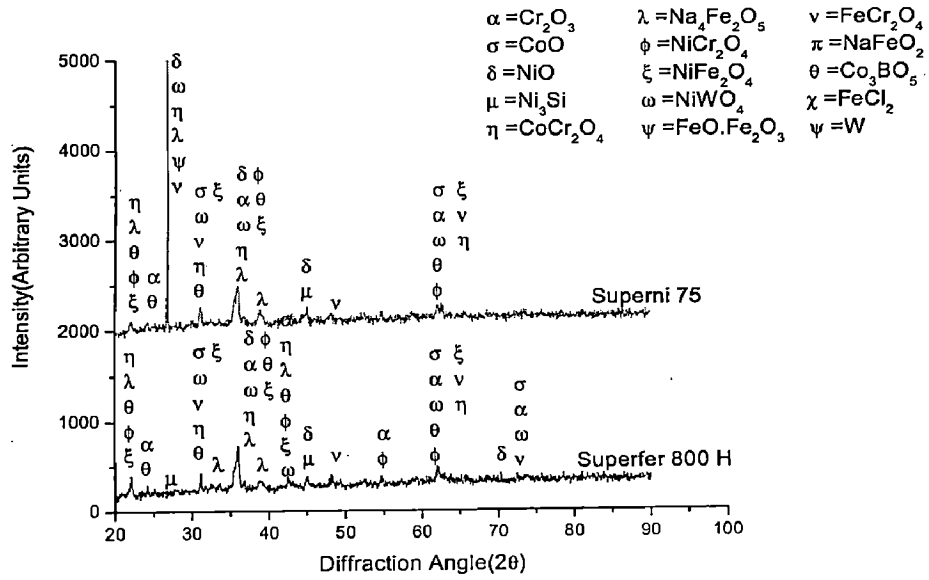


Fig5.11 XRD of coated superalloys in presence of molten salt environment

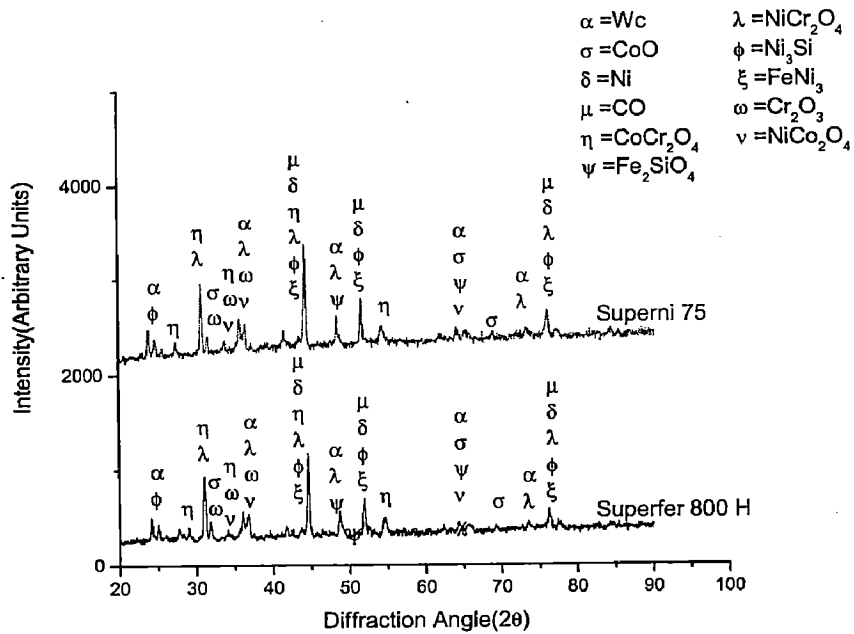


Fig 5.12 XRD of coated superalloys in presence of simple air oxidation environment

5.2.2.2 SEM Analysis of Coating

WC-NiCrFeSiB thermal spray coatings have an extremely complex microstructure, which is dependent on a number of factors relating to the powder feedstock, the processing method and the application conditions. An SEM image of an as-sprayed WC-NiCrFeSiB coating (Fig.5.13) indicates that the coating is massive and free of cracks. One can see negligible pores and oxide inclusions in the coating structure. There are globular melted particles in the matrix of a partially melted layer. There are some partially melted or unmelted particles can be seen on some areas the surface. These particles are identified in the coating by their size and near-spherical morphology similar to that shown in fig 5.5.

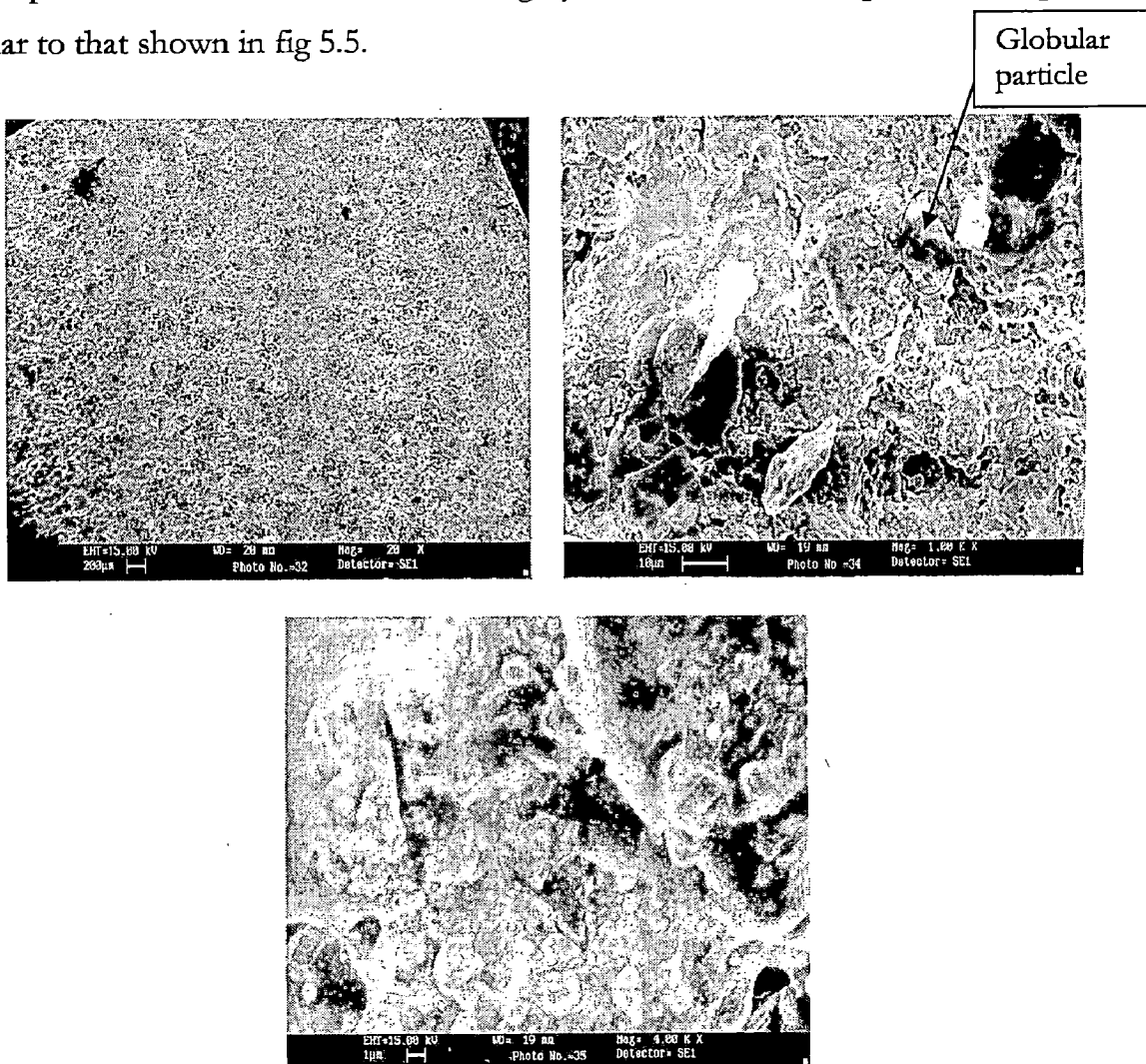


Fig 5.13 SEM of as sprayed coating on Superfer 800 H

5.2.2.3 SEM Analysis Of Scale

SEM micrographs of the corroded coated superalloy specimens in presence of salt environment, showing surface morphology after cyclic hot corrosion for 50 cycles at 800 °C, are shown in Fig.5.14 & 5.15. Micrographs of both the coated superalloy in presence of salt after cyclic hot corrosion for 50 cycles at 800 °C indicate the formation of continuous scale. SEM analysis of white areas, which believed to be the upper scale, reveals that Tungsten is the predominant phase. At higher magnification it looks like a hairy structure. This may be due to presence of WC. Chlorine generated by the dissociation of NaCl reacts with alloying elements such as chromium, nickel, iron and boron forms highly volatile metal chlorides, which diffuse out of the scale, react with oxygen present near the scale by releasing chlorine, and forming a discontinuous, and loose oxide scale.

Corroded coated superalloys after oxidation shows almost negligible corrosion attack. Fe base and Ni base superalloys shows almost similar SEM micrographs. This can also be seen from bar chart of cumulative weight gain of all the specimens(Fig6.1). The SEM analyses (Figure 5.16 and 5.17) reveal that the morphology of the coating did not considerably change during the corrosion exposure.

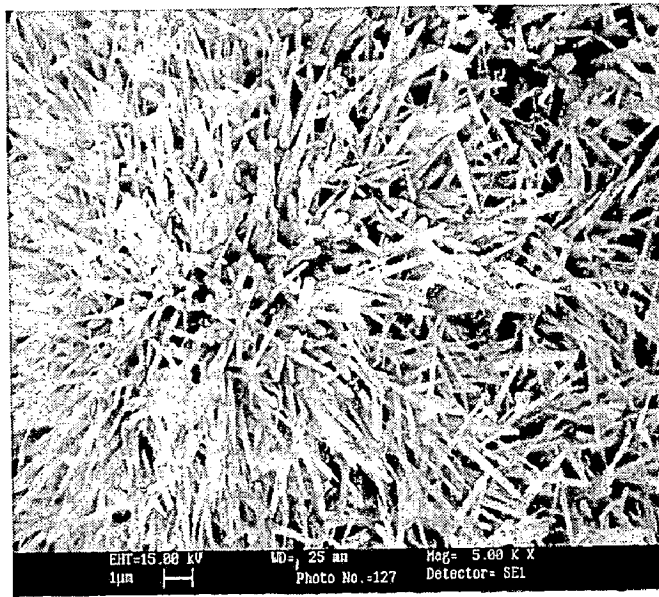
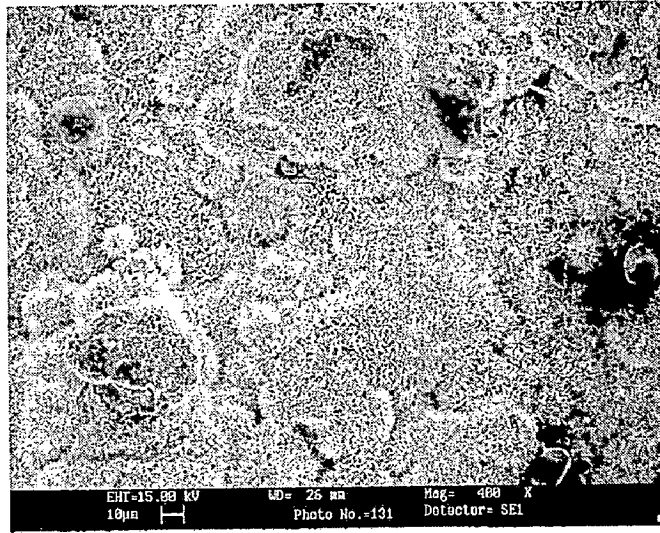


Fig 5.14 SEM of coated Superfer 800 H after corrosion in molten salt environment of 75%Na₂SO₄ + 25%NaCl

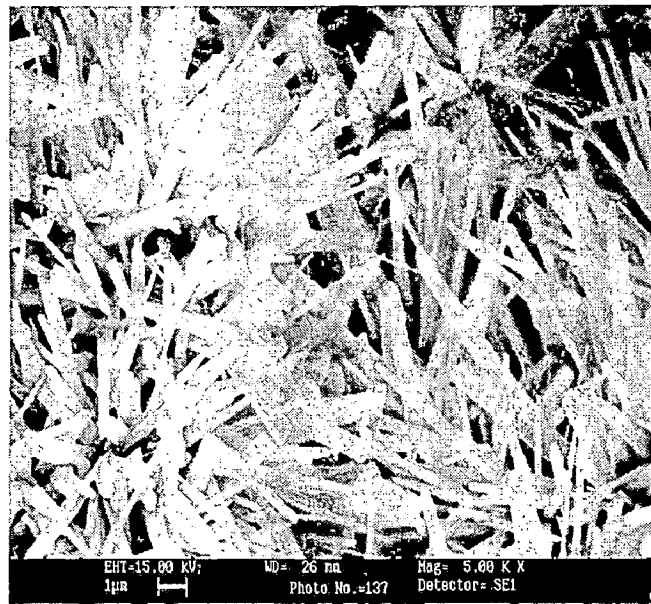
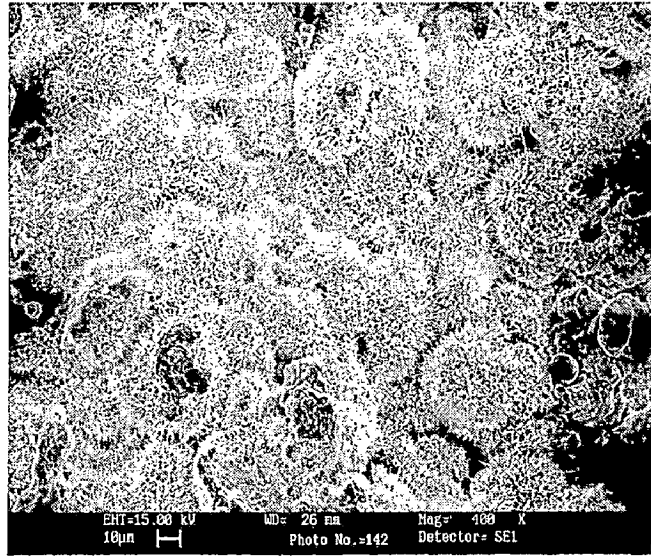


Fig 5.15 SEM of coated Superni 75 after corrosion in molten salt environment of 75%Na₂SO₄ + 25%NaCl

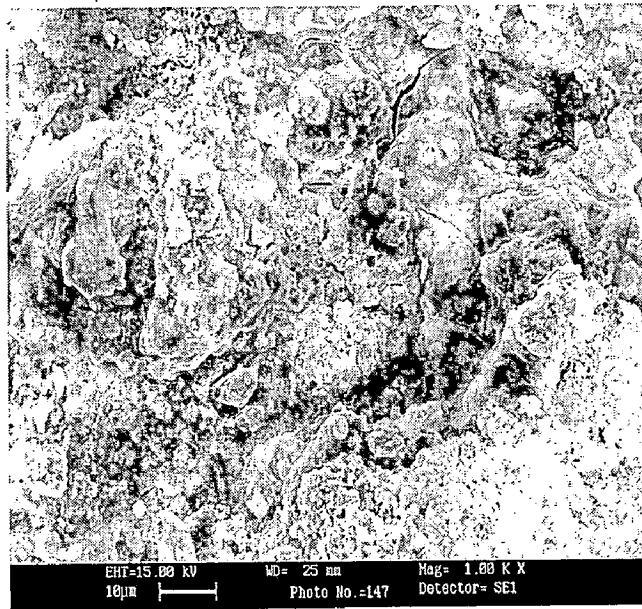
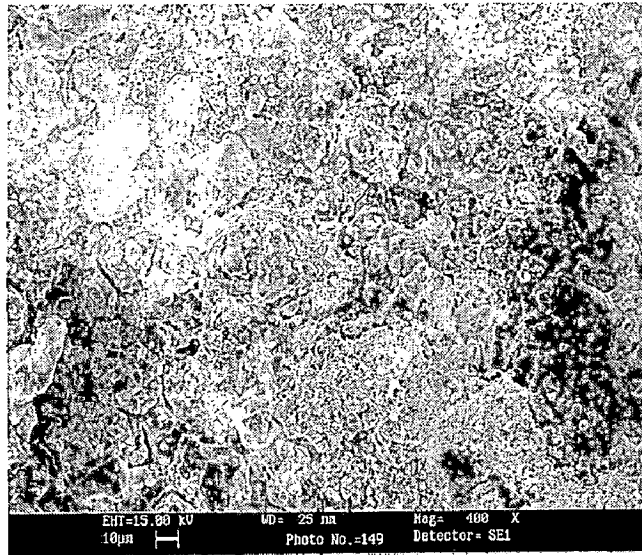


Fig 5.16 SEM of coated Superfer 800 H after corrosion in simple air oxidation environment

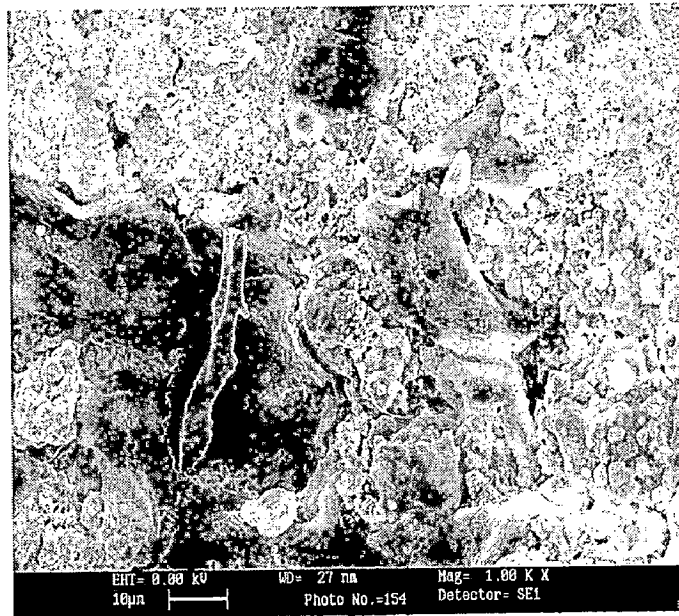
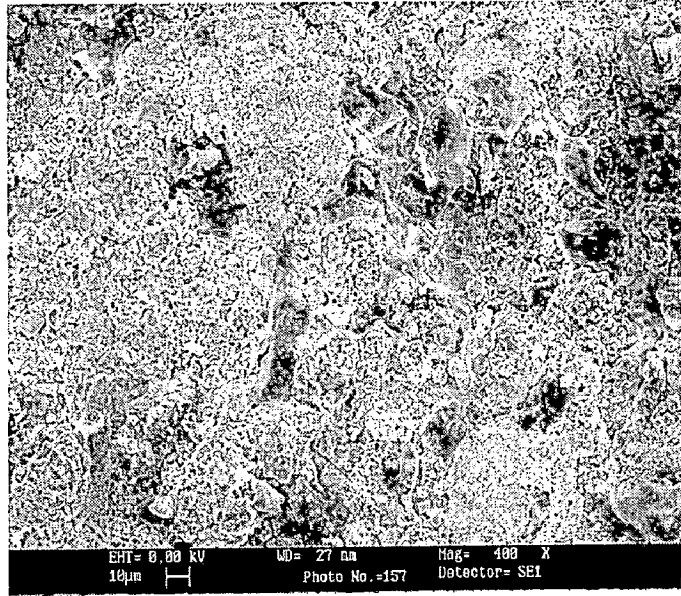


Fig5.17 SEM of coated Superni 75 after corrosion in simple air oxidation environment

5.2.2.4 Cross-sectional analysis of the oxide scales

The hot corroded samples were cut in cross-sections and mounted in transparent mounting resin, mirror polished and carbon coated to facilitate X-ray mapping of the different elements present across the scale. X-ray mappings for WC-NiCrFeSiB coated Superni 75 after 50 cycles of hot corrosion in an environment of 75% Na₂SO₄-25%NaCl at 800 °C (Fig. 5.23) indicate the formation of a scale containing mainly tungsten, nickel, chromium and cobalt. Iron is also present throughout the scale. Tungsten rich splats are present in the scale containing chromium, nickel and cobalt at the splat boundaries. Iron shows a relatively higher concentration near to the coating-substrate interface. From fig 5.18 scale thickness measured is 35.6 μm and in fig 5.19 scale thickness is 39.4μm.

EPMA of WC-NiCrFeSiB coated superfer 800 H after air oxidation(fig5.24) also shows the formation of tungsten splats and chromium, nickel and cobalt at the splat boundaries. In this fig 5.24 aluminum is also presents throughout the scale.

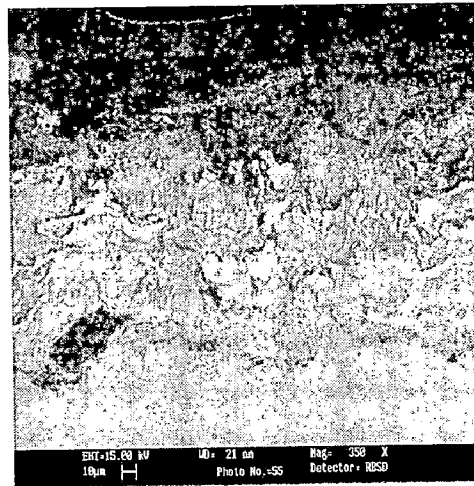


Fig5.18 BSE images of coated Superfer 800 H after corrosion in molten salt environment of 75%Na₂SO₄ + 25%NaCl

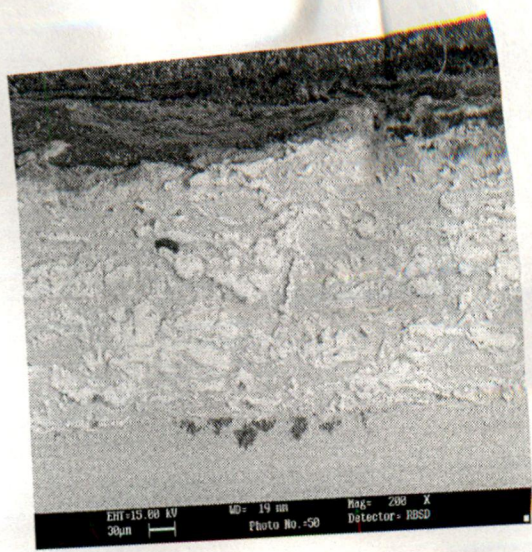


Fig5.19 BSE images of coated Superni 75 after corrosion in molten salt environment of $75\%Na_2SO_4 + 25\%NaCl$

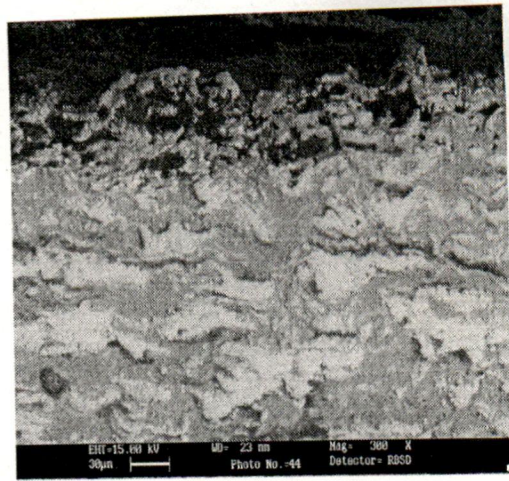


Fig5.20 BSE images of coated Superfer 800 H after corrosion in simple air oxidation environment

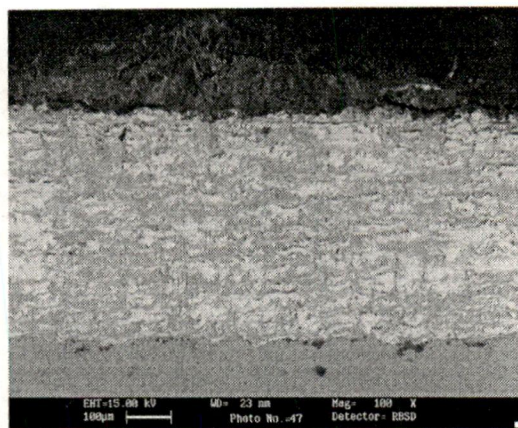


Fig5.21 BSE images of coated Superni 75 after corrosion in simple air oxidation environment

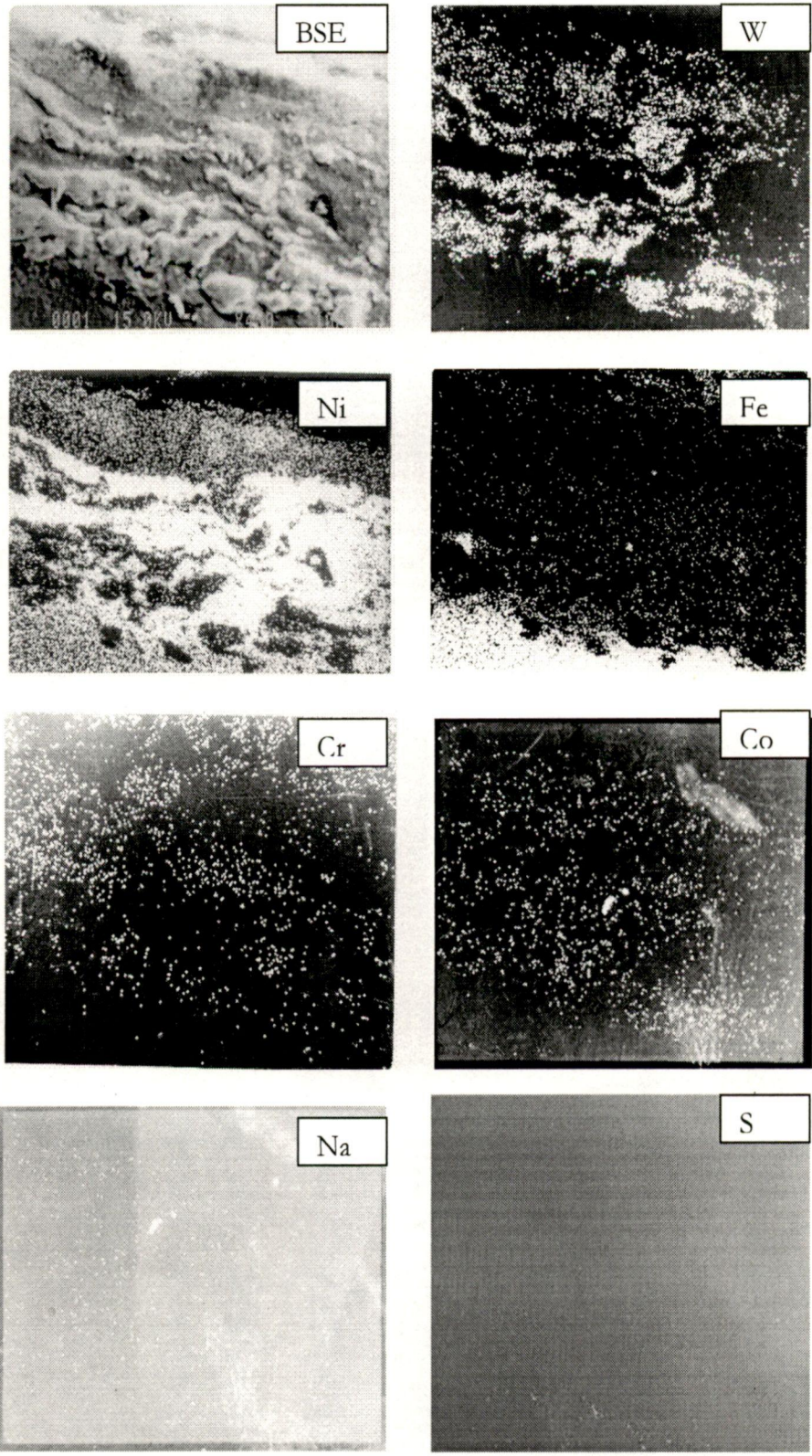


Fig 5.22 EPMA of corroded WC-NiCrFeSiB coated Superfer 800 H in presence of molten salt environment.

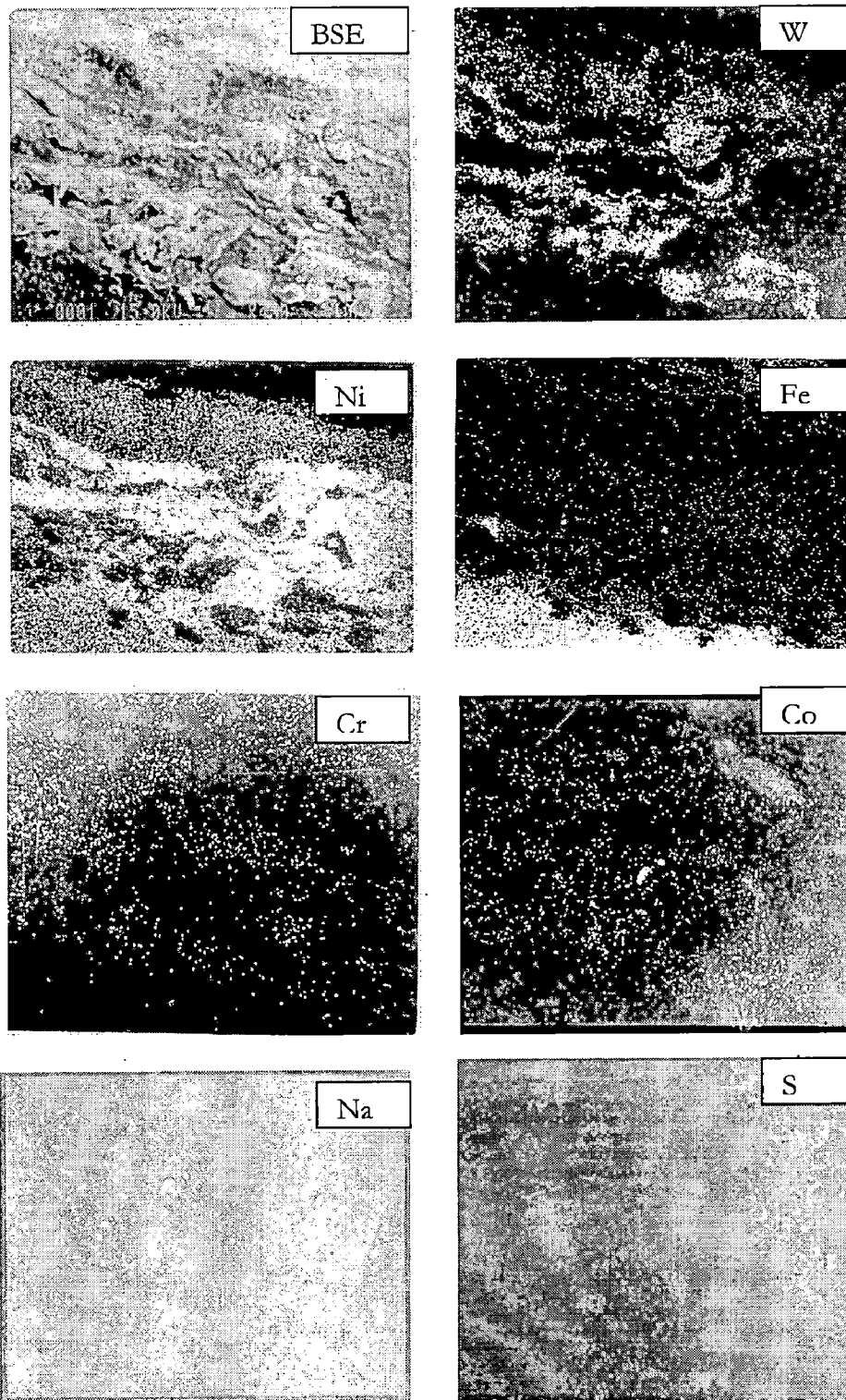


Fig 5.22 EPMA of corroded WC-NiCrFeSiB coated Superfer 800 H in presence of molten salt environment.

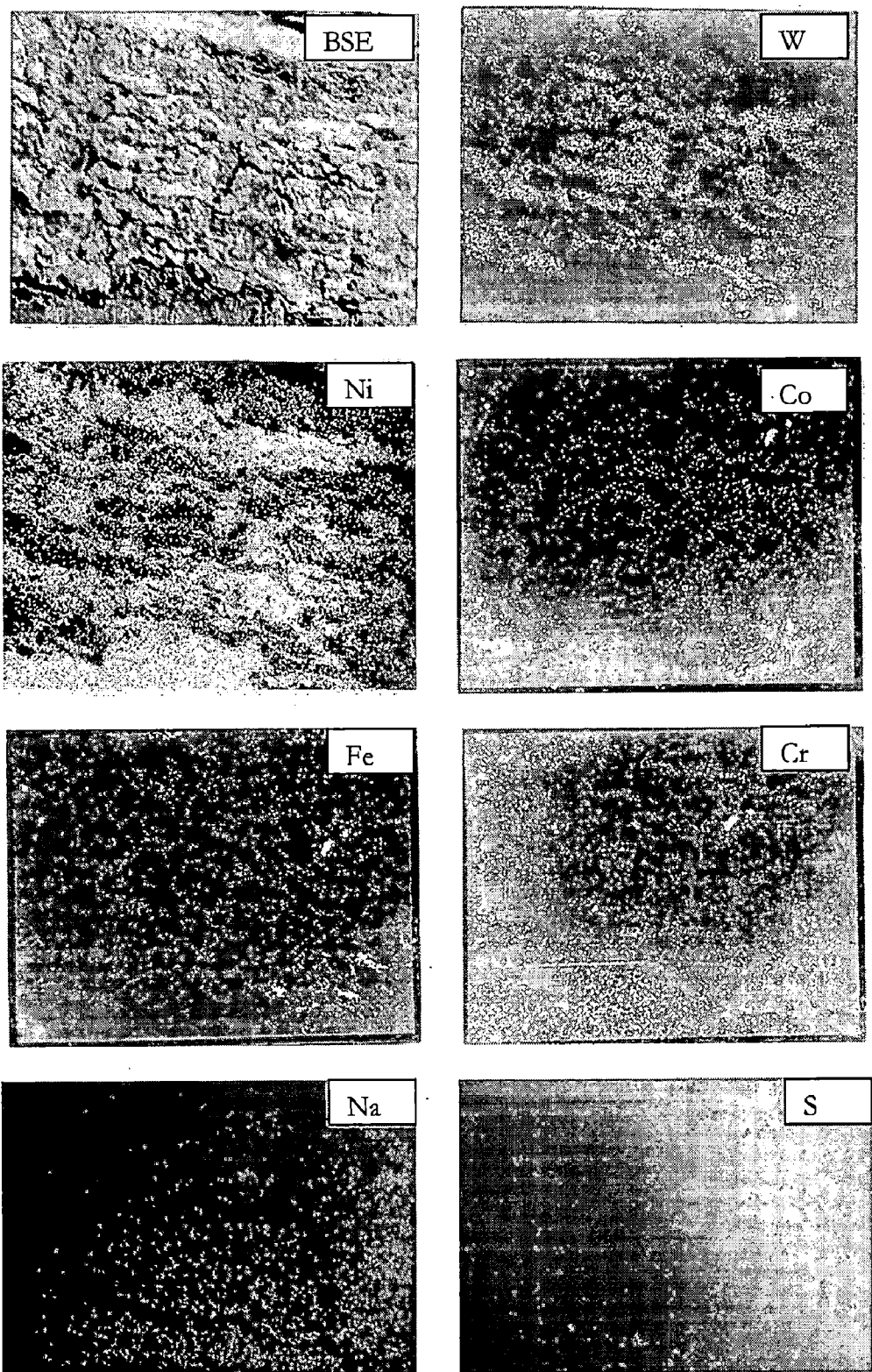


Fig5.23 EPMA of corroded WC-NiCrFeSiB coated Superni 75 in presence of molten salt environment.

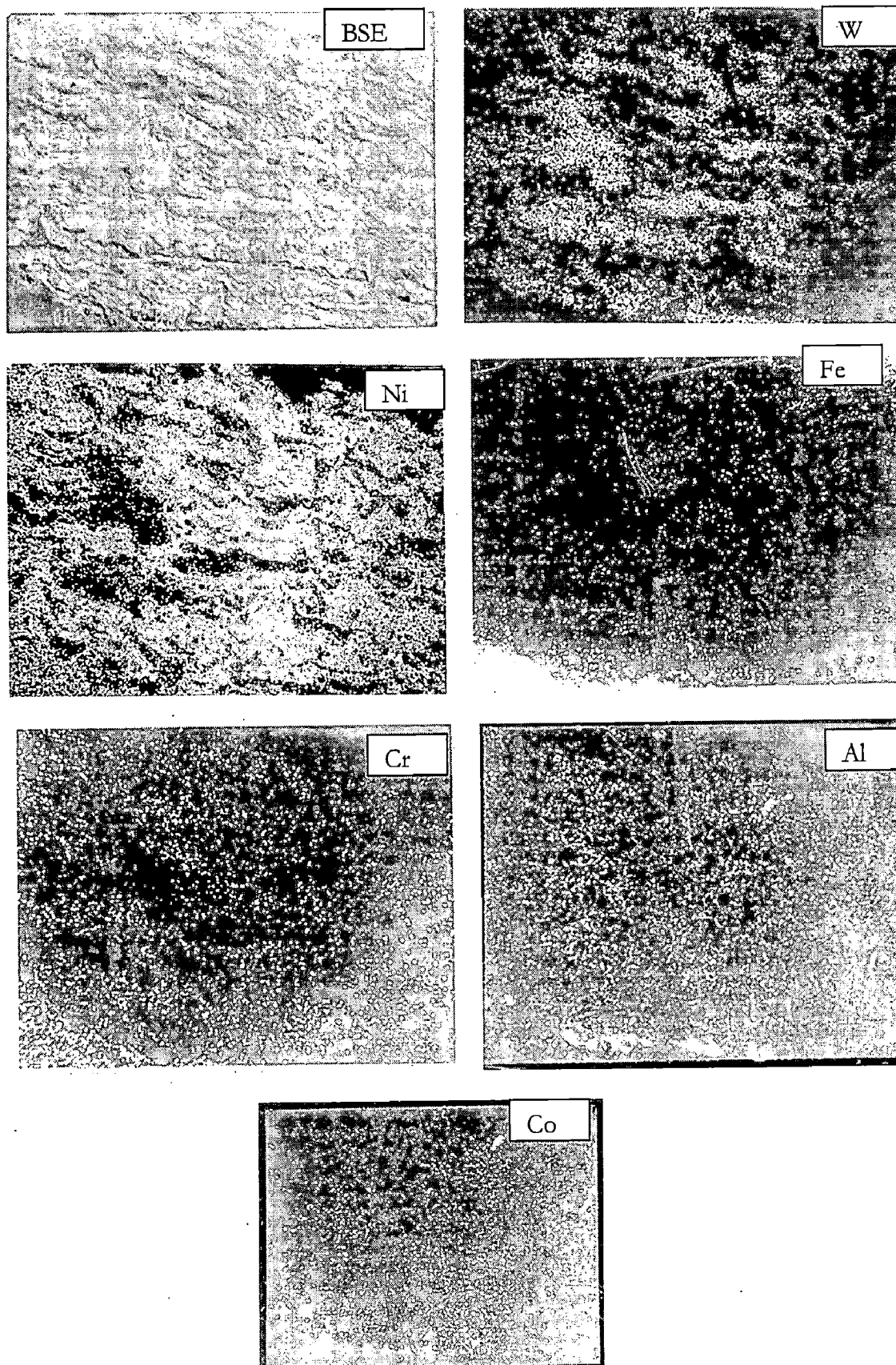


Fig5.24 EPMA of corroded WC-NiCrFeSiB coated Superfer 800 H in presence of simple air environment

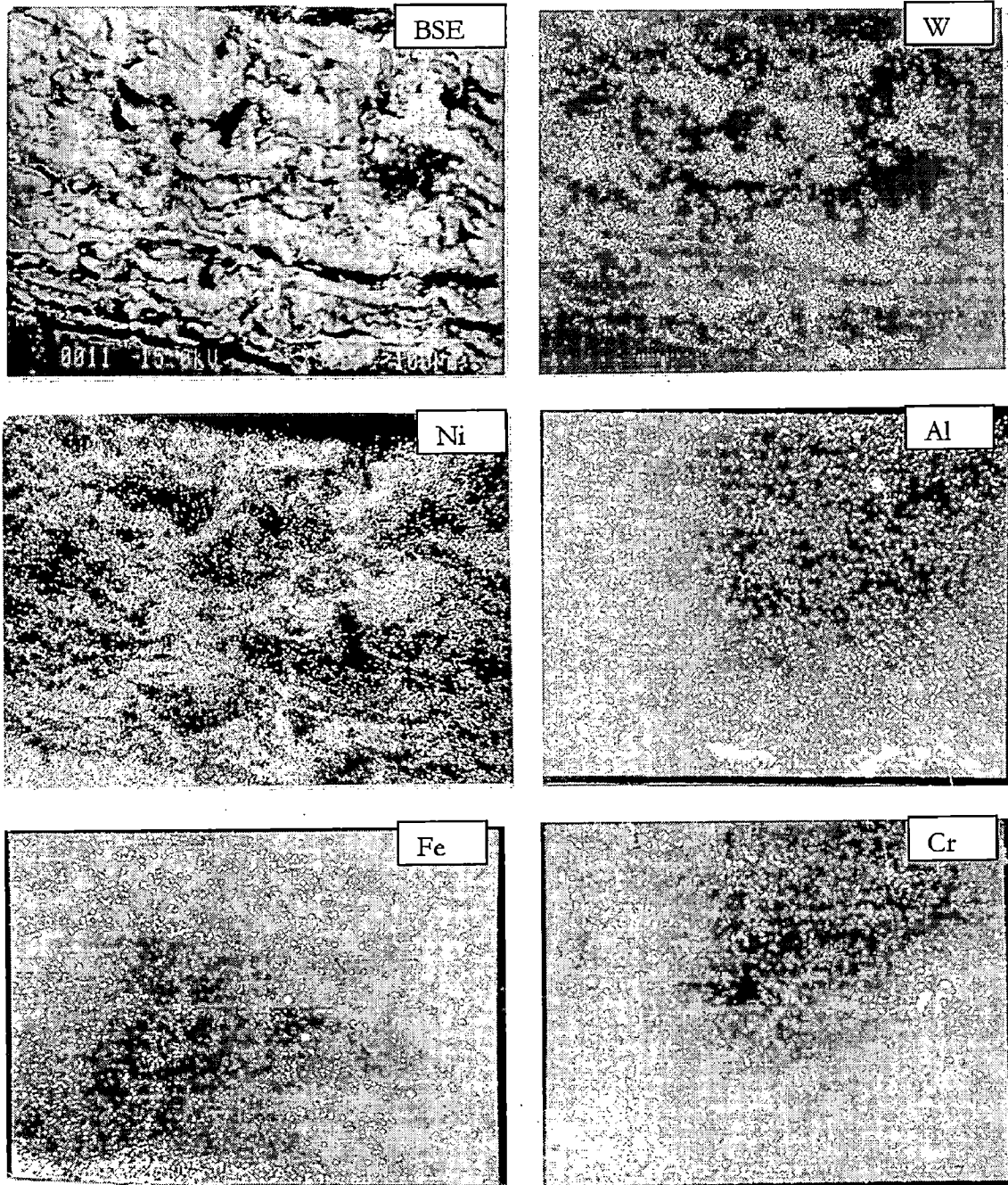


Fig5.25 EPMA of corroded WC-NiCrFeSiB coated Superni 75 in presence of simple air environment

Uncoated Superalloys

In general, the superalloys under study i.e. Superfer 800H and Superni 75 have shown good oxidation resistance.. The weight gain for the former case is about 2 times that for the latter case. Based on thermogravimetric data, the oxidation rate of Superfer 800H seems to be greater than that of Superni 75 and therefore it can be inferred that the relative oxidation resistance of Superni 75 is greater than that of Superfer 800H. The $(\text{weight}/\text{area})^2$ plots for the uncoated superalloys Superfer 800H shows the deviation from the parabolic rate law and Superni 75 indicate the conformance to parabolic rate law(fig5.2). The superior corrosion resistance shown by the Ni-based superalloys might be ascribed to the formation of Ni oxide which acts as a diffusion barrier for the oxidizing species as has been reported by Goebel JA and Pettit FS [17]. Malik [28] has also reported a similar sequence for the hot corrosion rates of Ni- and Fe-based superalloys based on the weight change data for 30 cycles.

As discussed by Prakash et.al. Cr forms a protective layer in the respective oxide scales after 50 cycles of oxidation.[12] The continuous chromia layer in turn might have blocked the diffusion of any species through it to reach the substrate superalloys and hence provide oxidation resistance to the base alloy. The weight gain graph, shows that the weight gained by bare superalloys increases continuously, although the rate of increase is relatively high during the initial period of exposure.

Intensive spalling/sputtering of the scale of the Superfer 800 H bare superalloys can be attributed to severe strain developed due to the precipitation of Fe_2O_3 from the liquid phase and interdiffusion of intermediate layers of iron oxide as has been reported by Sachs [46]. Further, the presence of different phases in a thin layer might impose severe strain on the film, which may result in cracking and peeling of the scale. The cracks may have allowed the aggressive liquid phase to reach the metal substrate. Diffusion of iron across the coating–substrate interface may have contributed to the better adhesion of the coatings.



Coated Superalloys

The weight gain data for the WC-NiCrFeSiB coated superalloys shows that the coating has been successful in reducing the overall weight gain in all cases (fig6.1). The parabolic rate constants for the uncoated superalloys are found to be greater than those for the coated superalloys in all cases. Further, all the coated superalloys showed parabolic oxidation behaviour up to 50 cycles in the given environment. Hence, it can be inferred that the necessary protection is provided by the WC-NiCrFeSiB coatings to the Ni and Fe-based superalloys in the given molten salt environment. The protection from hot corrosion might be due to the oxides of chromium and nickel and a spinel of nickel and chromium present in the top scales of coated superalloys, as revealed by XRD analysis. The presence of these phases in the scale of coated superalloys is further supported by the EPMA analyses. The oxides formed along the splat boundaries of the coatings might have acted as diffusion barriers to the inward diffusion of corrosive species. The scales formed on WC-NiCrFeSiB coated superalloys were observed to be dense and compact, without any spallation/ sputtering or peeling of the scale. Wang et al. [35] reported that addition of silicon and boron can promote the formation of continuous and dense scale in the initial corrosion stage and improve the adherence of the outer scale to the coating in the subsequent hot corrosion process. BSE images of WC-NiCrFeSiB superalloys shows that molten salt is not able to penetrate upto the substrate and coating remains adherent to the substrate.

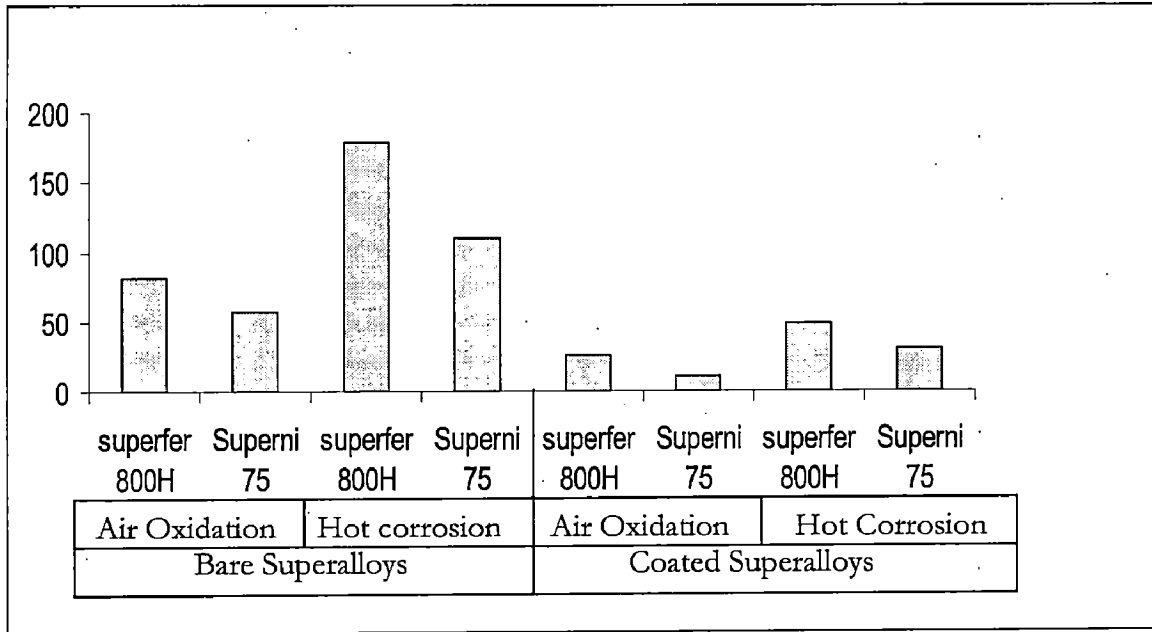


Fig 6.1 Cumulative weight gain of the Specimens having

Coating – Wc-NiCrFeSiB

Superalloys – Superfer 800 H
and Superni 75

Environments – 75% Na₂SO₄ + 25% NaCl
and air

Temperature – 800 °C

- Wc-NiCrFeSiB coatings have been successfully developed using a HVOF process. The coatings have been applied to Ni- and Fe-based superalloy substrates. WC-NiCrFeSiB coating indicates that the coating is massive and free of cracks, having coating thickness in the range of 250-310 μm .
- Fe-based uncoated superalloy Superfer 800H shows the maximum weight gain, whereas bare Superni 75 shows the minimum among all the superalloys in both the environments (with or without salt). The weight gain of Superni 75 after 50 cycles is nearly one-third of that of Superfer 800H.
- The coated superalloys in all cases show a much lower weight gain than the uncoated specimens in the given molten salt environment. The WC-NiCrFeSiB coating provides the maximum hot corrosion resistance to Superni 75 and has been found successful in reducing the weight gain by 80% of that gained without a coating.
- HVOF sprayed Wc-NiCrFeSiB coating improve the hot corrosion resistance of the Superfer 800 H and Superni 75 in the given conditions. The formation of oxides along the splat boundaries and within open pores of the coatings might have acted as diffusion barrier to the inward diffusion of corrosive species.
- The spallation and peeling of oxide scale was negligible for the Wc-NiCrFeSiB coating.
- The WC-NiCrFeSiB coating is very effective against hot corrosion and can be applied for boilers and turbines in marine environment.

SUGGESTIONS FOR FUTURE WORK

1. Studies may be conducted in actual industrial environments to investigate the corrosion behaviour and also of the coating developed by other methods (other than HVOF). Some other coating composition may also be tested.
2. High temperature erosion behaviour of the coatings may also be investigated.
3. The characterization of the products formed on the surface during studies and to understand the mechanism of corrosion, the analysis can be done by using EDAX analysis.
4. Attempts can be made to investigate the useful life of these coated superalloys by extrapolation of the laboratory data by mathematical modeling.
5. Cost effectiveness analysis should be done for different types of coatings.

1. T.S Sidhu, R.D. Agrawal and S. Prakash, *Hot corrosion of some superalloys and role of high-velocity oxy-fuel spray coatings—a review*, Surface & Coatings Technology, 198 (2005) 441– 446
2. R.A. Rapp and Y.S. Zhang, *Fundamental studies of hot corrosion*, Journal of materials processing, 47 (1994 Dec.) 47-55
3. N. Eliaz, G. Shemesh, and R.M. Latanision, *Hot corrosion in gas turbine components*, Engineering Failure Analysis 9(2002) 31-43
4. G. S. Frankel, *Corrosion Science in the 21st Century*, The Journal Of Corrosion Science And Engineering, Volume 6 Paper C028
5. V.A.D. Souza, A. Neville, *Corrosion and synergy in a WC Co Cr HVOF thermal spray coating— understanding their role in erosion–corrosion degradation*, Wear 259 (2005) 171–180
6. V. Stoica, R. Ahmed, T. Itsukaichi, S. Tobe, *Sliding wear evaluation of hot isostatically pressed (HIPed) thermal spray cermet coatings*, Wear 257 (2004) 1103–1124
7. Goebel JA and Pettit FS., *Na₂SO₄ induced accelerated oxidation (hot corrosion) of nickel base superalloys*, Metall Trans 1 (1970) 43-54.
8. D. Deb, S.R. Iyer and V.M. Radhakrishnan, *A comparative study of oxidation and hot corrosion of a cast nickel base superalloy in different corrosive environments*, Materials Letters, 29 (1996) 19
9. Zhu Rizhang, Guo Manjiou,t and Zuo Yu, *A Study of the Mechanism of Internal Sulfidation- Internal Oxidation during Hot Corrosion of Ni-Base Alloys* , *Oxidation of Metals*, Vol. 27, Nos. 5/6, 1987
10. A.U. Malik and S. Ahmad, *Na₂SO₄-Induced corrosion of some Nimonic Alloys at 650 to 1000 degree C*, Zeitschrift fuer Metallkunde, 74(12) (1983) 819

11. I. Gurrappa, *Hot Corrosion Behavior of CM 247 LC Alloy in Na₂SO₄ and NaCl Environments*, *Oxidation of Metals*, Vol. 51, Nos. 5/6, 1999
12. J.C. Tan, L. Looney and M.S.J. Hashmi, *Component repair using HVOF thermal spraying*, *Journal of materials processing technology*, 92–93 (1999) 203
13. Charng- Cheng Tsaur C.Rock, Chaur-Jeng Wang and Yung-Hua Su, *The Hot Corrosion Of 310 Stainless Steel with pre-coated NaCl/Na₂SO₄ mixtures at 750 °C*, *Materials chemistry and Physics* 89(2005) 445-453, 1 October 2004
14. J. Koutsky, *High velocity oxy-fuel spraying*, *Journal of Materials Processing Technology*, 157–158 (2004) 557–560
15. *Thermal Spray Coating Selection*, EM 1110-2-3401, 29 Jan 99
16. Stringer J., *High-temperature corrosion of superalloys*, *Materials Science Technology*, 3(7) (1987) 482-93
17. Jeffrey H. Boy, Ashok Kumar, *Cavitation- and Erosion-Resistant Thermal Spray Coatings*, USACERL Technical Report 97/118, July 1997
18. *Introduction to Thermal Spray Processing*, Hand Book Of Thermal Spray Technology. From www.asminternational.org/bookstore.
19. H. Herman, S. Sampath and R. McCune, *Thermal spray: Current status and future trends*, *MRS Bulletin*, 25 (7) (2000) 17.
20. T. S. Sidhu, S. Prakash and R. D. Agrawal, *Hot corrosion and performance of nickel-based coatings*, *Current Science*, Vol. 90, NO. 1, 10 JANUARY 2006
21. R. Mevrel, *State of the art on high-temperature corrosion-resistant coatings*, *Materials Science Engineering A*, 120 (1989) 13
22. Hazoor Singh Sidhu, Buta Singh Sidhu, S. Prakash, *The role of HVOF coatings in improving hot corrosion resistance of ASTM-SA210 GrA1 steel in the presence of Na₂SO₄*

V_2O_5 salt deposits, Surface & Coatings Technology xx (2005) xxx–xxx

23. Kari Korpiola, High Temperature Oxidation of Metal, Alloy, and Cermet Powders In HVOF Spraying Process (Doctoral Thesis), Espoo 2004
24. J.R. Nicholls, D.J. Stephenson, High temperature coatings for gas turbines, Surface Engineering, 22 (1991) 156.
25. K.L. Luthra, Kinetics of the Low Temperature Hot Corrosion of Co–Cr–Al Alloys, Journal of Electrochem Soc, 132 (6) (1985) 129
26. T.S. Sidhu, S. Prakash, R.D. Agrawal. Hot corrosion studies of HVOF sprayed Cr_3C_2 –NiCr and Ni–20Cr coatings on nickel-based superalloy at 900 °C, Surface & Coatings Technology xx (2006) xxx–xxx
27. Otsubo F, Era H and Kishitake K, Structure and Phases in Nickel-Base Self-Fluxing Alloy Coating Containing High Chromium and Boron, Journal of Thermal Spray Technology, 91 (2000) 107.
28. Bornstein N.S. and Decrescente M.A., The role of sodium in the accelerated oxidation phenomenon termed sulfidation, Metall Trans, 2 (1971) 2875-83.
29. M. Mobin, A. U. Malik and Sultan Ahmad, High Temperature Interactions Of Metal Oxides With NaCl, Journal of the Less-Common Metals, 160 (1990) 1- 14
30. V. Nagarajan, J. Stringer and D. P. Whittle, The Hot Corrosion Of Cobalt-Base Alloys In A Modified Dean's Rig--I. Co-Cr, Co-Cr-Ta AND Co-Cr-Ti Alloys, Corrosion Science, Vol. 22, No. 5, pp. 407-427, 1982
31. Goebel JA, Pettit FS and Goward GW, Mechanisms for the hot corrosion of nickel-base alloy, Metall Trans, 4 (1973) 261-78
32. F.S. Pettit, G.H. Meier, In: M. Gell, C.S. Kartovich, R.H. Bricknel, W.B. Kent, J.F. Radovich, Editors, "Oxidation and Hot corrosion of Superalloys", Superalloys, The Met. Soc. of AIME, Warrendale, PA(1984) p. 651

33. A.U. Malik, *Hot corrosion behaviour of some industrially important nickel-base alloys in presence of $Na_2SO_4(s)$ and $NaCl(s)$* , Zeitschrift fuer Metallkunde, 79(5) (1988) 285
34. T.S. Sidhu, S. Prakash, R.D. Agrawal, *Studies of the metallurgical and mechanical properties of high velocity oxy-fuel sprayed stellite-6 coatings on Ni- and Fe-based superalloys*, Surface & Coatings Technology xx (2005) xxx–xxx
35. D.W. Parker and G.L. Kutner, *HVOF-spray technology poised for growth*, Advanced Materials and Processes, 4 (1991) 68.
36. W-M. Zhao, Y. Wang, T. Han, K-Y. Wu and J. Xue, *Electrochemical evaluation of corrosion resistance of NiCrBSi coatings deposited by HVOF*, Surface Coating Technology 183 (2003)
37. Q.M.Wang, Y.N.Wu, P.L. Ke, H.T. Cao, J. Gong, C. Sun and L.S. Wen, *Hot corrosion behavior of AIP NiCoCrAlY(SiB) coatings on nickel base superalloys*, Surface Coating Technology, 186 (2004) 389